MOLECULAR ONCOLOGY 8 (2014) 178–195

available at www.sciencedirect.com

ScienceDirect

www.elsevier.com/locate/molonc

Collective migration of cancer-associated fibroblasts is enhanced by overexpression of tight junction-associated proteins claudin-11 and occludin

George S. Karagiannis[a,b], David F. Schaeffer[b,c], Chan-Kyung J. Cho[a,b], Natasha Musrap[a,b], Punit Saraon[a,b], Ihor Batruch[b], Andrea Grin[b], Bojana Mitrovic[b], Richard Kirsch[b], Robert H. Riddell[a,b], Eleftherios P. Diamandis[a,b,d,*]

[a]Department of Laboratory Medicine and Pathobiology, University of Toronto, Toronto, Ontario, Canada
[b]Department of Pathology and Laboratory Medicine, Mount Sinai Hospital, Toronto, ON, Canada
[c]Department of Pathology and Laboratory Medicine, University of British Columbia, British Columbia, Vancouver, Canada
[d]Department of Clinical Biochemistry, University Health Network, Toronto, Ontario, Canada

ARTICLE INFO

Article history:
Received 24 July 2013
Received in revised form
22 October 2013
Accepted 22 October 2013
Available online 8 November 2013

Keywords:
Colorectal cancer
Cancer-associated fibroblasts
Migration
Claudin-11
SILAC

ABSTRACT

It has been suggested that cancer-associated fibroblasts (CAFs) positioned at the desmoplastic areas of various types of cancer are capable of executing a migratory program, characterized by accelerated motility and collective configuration. Since CAFs are reprogrammed derivatives of normal progenitors, including quiescent fibroblasts, we hypothesized that such migratory program could be context-dependent, thus being regulated by specific paracrine signals from the adjacent cancer population. Using the traditional scratch assay setup, we showed that only specific colon cancer cell lines (i.e. HT29) were able to induce collective CAF migration. By performing quantitative proteomics (SILAC), we identified a 2.7-fold increase of claudin-11, a member of the tight junction apparatus, in CAFs that exerted such collectivity in their migratory pattern. Further proteomic investigations of cancer cell line secretomes revealed a specific signature, involving TGF-β, as potential mediator of this effect. Normal colonic fibroblasts stimulated with TGF-β exerted myofibroblastic differentiation, occludin (OCLN) and claudin-11 (CLDN11) overexpression and cohort formation. Subsequently, inhibition of TGF-β attenuated all the previous effects. Immunohistochemistry of the universal tight junction marker occludin in a cohort of 30 colorectal adenocarcinoma patients defined a CAF subpopulation expressing tight junctions. Overall, these data suggest that cancer cells may induce CLDN11 overexpression and subsequent collective migration of peritumoral CAFs via TGF-β secretion.

Non-standard abbreviations: CAF, cancer-associated fibroblast; CALD, caldesmon; CLN11, claudin 11; CM, conditioned media; ECM, extracellular matrix; EMT, epithelial-to-mesenchymal transition; ICC, immunocytochemistry; IGP, invasive growth potential; IHC, immunohistochemistry; LAMA3, laminin a3; LAMB1, laminin b1; MEHP, mono-(2-ethylhexyl) phthalate; MWL, mean wound length; NMC/DSA, number of migrating cells per default squared area; OCLN, occludin; PLAU, urokinase-type plasminogen activator; SILAC, stable isotope labeling with amino acids in cell culture; TGF-β, transforming growth factor-beta.

* *Corresponding author*. Mount Sinai Hospital, Joseph & Wolf Lebovic Center, 60 Murray St. [Box 32], Floor 6 – Room L6-201, Toronto, ON M5T 3L9, Canada. Tel.: +1 416 586 8443; fax: +1 416 619 5521.
E-mail address: ediamandis@mtsinai.on.ca (E.P. Diamandis).

1574-7891/$ – see front matter © 2013 Federation of European Biochemical Societies. Published by Elsevier B.V. All rights reserved.
http://dx.doi.org/10.1016/j.molonc.2013.10.008

1. Introduction

One of the many crucial steps in cancer formation is the interaction between cancer and stromal cells at the invasive margins of the continuously expanding neoplasia. The aggressiveness of a particular carcinoma has been shown to be heavily dependent on the ability of the malignant cells to recruit the surrounding stromal cells. One particular subgroup of stromal cells, the cancer-associated fibroblasts (CAFs), is often found at the cancer invasive front, and has recently emerged as key player in this interaction. CAFs share a similar phenotype with myofibroblasts observed during wound healing and most of the times, they comprise reprogrammed variants of the quiescent fibroblast population (Hanahan and Weinberg, 2011; Kalluri and Zeisberg, 2006). Accumulation of peritumoral CAFs is often associated with increased deposition of extracellular matrix (ECM) components, such as collagens, fibrin, proteoglycans and glycosaminoglycans, a lesion also known as "desmoplasia" or "desmoplastic reaction" (Kunz-Schughart and Knuechel, 2002).

CAF populations found in different types or subtypes of cancer or even within the same cancer may share different gene and protein expression signatures. This heterogeneity explains the identification of a plethora of CAF subtypes, which, most of the times, present with diverse functional properties. There have been two possible explanations for this diversity.

First, CAFs may be derived from a wide variety of other progenitor cells beyond the pure fibroblastic subpopulation. For instance, bone marrow-derived circulating cells and myeloid precursors are able to localize and proliferate in the peritumoral stroma, specifically contributing to the myofibroblasts of the desmoplastic response, as well as angiogenesis (Direkze et al., 2004; Russo et al., 2006). Of note, the phenotypic switching of endothelial cells seems to also be context-dependent, as various cytokines present in their microenvironment, such as transforming growth factor-β (TGF-β), have been shown to induce a biological program termed endothelial-to-mesenchymal transition (Potenta et al., 2008). Indeed, a significant proportion (up to 40%) of CAFs may share endothelial markers such as PECAM/CD31, which implies that they originate from an endothelial subpopulation (Potenta et al., 2008). Remarkably, a special case of the epithelial-to-mesenchymal transition (EMT) program, which is deployed by cancer cells to efficiently assist their invasive/migratory behavior, may sequentially lead to the formation of CAFs, given that a permissive microenvironment exists. For instance, Petersen et al. (2001) showed that breast cancer cells may typically undergo an EMT event that transforms them into myoepithelial cells and a subsequent transdifferentiation event, which results in the generation of a non-malignant stroma consisting of CAFs (Petersen et al., 2001, 2003).

Second, recent evidence suggests that during cancer progression, tumor cells are able to alter the characteristics of the adjacent stroma and create a supportive microenvironment in a context-dependent way. In other words, cancer cells are dynamically altered (i.e. their genetic background is constantly changing), which allows them to secrete a diverse repertoire of growth factors and paracrine signaling molecules, which, in turn, are able to shape the tumor microenvironment in their favor and address any new challenges encountered in the metastatic cascade (Elenbaas and Weinberg, 2001; Serini and Gabbiani, 1999).

We have previously proposed a model of CAF-directed metastatic progression, according to which CAFs are able to migrate within the tumor microenvironment and the tumor compartment in a cohort configuration by developing a specific migratory, adhesive and paracrine signaling machinery (Karagiannis et al., 2013, 2012b). In that model, we additionally claimed that the recruitment of such machinery is causatively associated with increased metastatic behavior of the cancer cells Consistent with previous observations (Elenbaas and Weinberg, 2001; Scheel et al., 2011), here we conclude that the development of such machinery should be dependent on microenvironmental signals originating from the cancer cells, further closing this paracrine feedback loop. To demonstrate this, we hypothesized that stimulation of normal fibroblasts with secreted factors originating from cancer cell lines of different genetic backgrounds would allow us to observe their different migratory behavior.

2. Experimental procedures

2.1. Reagents

The recombinant human TGF-β1, the pan-TGF-β neutralizing antibody and the tight junction inhibitor mono-(2-ethylhexyl) phthalate (MEHP) were purchased from Sigma–Aldrich. The active occludin-disrupting peptide LYHY and the corresponding control peptide LYQY were purchased from CanPeptide.

2.2. Cell culture

The human colon cancer cell lines HT29, SW480 and SW620, and the normal colonic fibroblast cell line 18Co, were obtained from the American Type Culture Collection (ATCC, Rockville, MD) and maintained in Dulbecco's Modified Eagle's Medium (DMEM), supplemented with 10% Fetal Bovine Serum (FBS), and 1% penicillin/streptomycin, in a humidified atmosphere of 5% CO_2, at 37 °C. All experiments were conducted before passage #8 from the initiation of all cultures. For stimulations, conditioned media (CM) from 18Co, HT29, SW480 and SW620 cells were generated in serum-free (SF) conditions. Briefly, the cells were seeded at 50% confluence in T175 flasks, in DMEM with 10% FBS for 12 h to allow for adherence and proliferation. Then, the flasks were washed with phosphate buffered saline (PBS) twice and SF medium (chemically-defined Chinese hamster ovary; CDCHO) was added in the cultures for 2 days. Then, all the media were collected, centrifuged at 1500 rpm for 5 min to remove dead cells and were concentrated 4 times, using a 5 kDa membrane cut-off. Concentrated media were rediluted 4 times, in fresh SF medium, to enrich for nutrients, and subsequently filter-sterilized through a 0.22 μm membrane cut-off. For the SILAC experiment, labeled SF stimulation media were generated to not disturb the metabolic incorporation of the heavy and light amino acid isotopes.

For details in the labeling of cells, see relevant chapter in Material and Methods section. We observed that stimulation of normal fibroblasts with labeled media induced similar *in vitro* responses as the non-labeled media, and cell death was not significantly altered (data not shown).

2.3. Cell proliferation assay

For the assessment of cell proliferation, the crystal violet assay was performed, as previously described (Karagiannis et al., 2012a).

2.4. Cell scratch assay

Normal fibroblasts were seeded in six-well plates. After forming confluent monolayers, a pipette tip was used to create a single straight scratch on the well and they were carefully rinsed 3 times with 4–5 mL of PBS to remove detached and dead cells. After washing, the experimental conditions and treatments were applied on the wells, in at least 3 biological replicates. The specifics for the experimental conditions are described in the corresponding sections. The wells were left for 8–48 h, depending on the measurable parameter and then all media were removed, cells were washed once with PBS and fixed with 10% formalin for 20 min. After fixation, crystal violet solution (0.05%) was applied in the wells (~3 mL) for 30 min. Then, the staining dye was removed; cells were washed twice with PBS and examined under light microscopy. Several images per condition and per replicate were taken, which were then uploaded into ImageJ software for further analysis.

Mean wound length (MWL): in each image, a total of 50 lines were drawn; the lines were perpendicular to the wound axis and connected the edges of two fibroblasts lining the opposite sites of the wound. All lines were measured and the mean wound length in each condition was estimated. In order to ignore zoom-preference biases, all MWLs were graphed relatively to the initial wound length.

Number of migrating cells/default squared area (NMC/DSA): in each image three randomized squared areas, corresponding to 1/16th of the image's surface, were placed in the wound gap and migrating cells were counted. Cells that were not estimated as migrating cells, i.e. cells that were still attached to the wound edges, were ignored. There was an attempt to obtain more than 20 measurements per condition. The squared area and zoom-preference were the same in all conditions examined, to avoid the need for cell count normalization. Average numbers of migrating cells were calculated. Data were graphed as average NMC/DSA.

Invasive growth potential (IGP): in each image, the distance of the biggest fibroblast collective from the sprouting point to the tip cell was measured. It was made certain that the collective had not detached from the wound edge. The length was illustrated as a line, vertical to the wound axis. Relative measurements were performed between the conditions to avoid zoom-preference biases. Data were graphed as average IGP from 10 to 15 collectives from different images of the same condition.

Positive direction-sensing: in each image, a randomized method for selection of 10 edge cells was applied. These cells were then examined by a blinded observer for presence of cytoplasmic protrusions and front-to-rear polarity axis, within the 120° angle facing the wound. For this assessment, the Y method was followed; specifically, the Y schematic was placed in the nucleus of each individual cell in a vertical reorientation towards the wound axis and the presence of protrusions or front axis was evaluated in each of the three segments. A minimum of 100 cells per condition were evaluated and the results were graphed as percentage of cells with positive direction-sensing. Because there are three possible orientations using this method, it was assumed that 33% of the cells could randomly obtain this reorientation, immediately after the generation of the scratch. Therefore, the 33% was considered as a cut-off to accept significant percentages of reorientation.

2.4.1. Assessment of collectivity of migration

Following principles by Rorth (2009) (Rorth, 2009), we assessed collective migration as the type of migration where there is a synchronous low NMC/DSA, with increased IGP and a significant reduction in the MWL. Less collective and more individual cell migration was characterized with the exactly opposite metrics.

2.5. Collagen gel contraction assay

Rat tail tendon collagen (RTTC), a type I collagen, was purchased from BD Biosciences. The collagen gels were prepared after mixing RTTC, distilled water, 4X DMEM, 10X gel contraction buffer (200 mmol/L HEPES, 2.2% $NaHCO_3$, 0.05 N NaOH), FBS, crystal violet and cells. The final concentrations were: 1.5 mg/mL RTTC, 1X DMEM, 1X gel contraction buffer, 1.5% FBS, 0.01% crystal violet and 6×10^5 cells/mL. A total of 0.5 mL of this mixture was mounted on 24-well plates and was then left to polymerize at 37 °C for 30 min. After polymerization, the gels were released from the plate with a scalpel and transferred into 6-cm tissue culture dishes. The surface area of the gels was measured as a relative value compared with that of a 6-cm dish. These values were normalized to that of the control gel at 0 h.

2.6. Immunostaining

For immunocytochemistry, the mouse monoclonal antibodies against either a-SMA or claudin-11 were utilized and our previously published method (Karagiannis et al., 2012a) was followed. All staining conditions were performed in three replicates and repeated in two independent experiments. Stimulations were performed for 48 h. For protein expression scoring, three blinded observers provided individual scores for a-SMA and CLDN11 immunoreactivity in 10 optical fields per replicate; those were selected through a randomized template of squared areas applied onto each image. The data were presented as mean values with their standard deviations. All quantifications were performed in a microscope objective 100X.

For immunohistochemistry, we randomly selected a patient cohort of 30 invasive colon cancers, encompassing well-, moderately-, and poorly-differentiated adenocarcinomas ($n = 3$, 16 and 11 respectively). Staining was carried out with avidin-biotinylated peroxidase complex (ABC Elite

Kit, Vector Laboratories) on a LabVision 720 Autostainer (Labvision, Fremont, CA) using 1X TBS-Tween rinse and wash solution. 4 μm thick paraffin sections, mounted on positively charged glass slides, and baked at 60° for a minimum of 60 min. Sections were then immersed in xylene, followed by graded alcohols, at 10 min per solution. Antigen retrieval involved heating slides in a citrate (pH 6.0) buffer in either a microwave or a pressure cooker. Sections were then incubated with the primary antibodies occludin (rabbit polyclonal; dilution 1:200; Sigma), α-smooth muscle actin (Clone 1A4, dilution 1:200, Dako), h-caldesmon (h-CD; dilution 1:400; Dako), laminin-alpha3 (rabbit polyclonal; dilution 1:300; Sigma), laminin-beta1, (rabbit polyclonal; dilution 1:400; Sigma), and beta-catenin (clone 14; 1:200; BDBioscience). Diaminobenzidine hydrochloride solution with hydrogen peroxide (Sigma) was the chromogen. An appropriate internal positive control was validated in each case and negative controls were performed by omitting the primary antibody step.

2.7. Proteomic datasets and bioinformatics

Protein datasets from proteomic analysis of HT29, SW480 and SW620 CM were retrieved from our previously published study (Karagiannis et al., 2012a). A normalized spectral counting method was utilized, as previously described (Collier et al., 2010), for purposes of measuring the relative abundance of TGF-β1 in these datasets. Gene expression meta-analysis for claudin-11 was performed using Genevestigator, as previously described (Karagiannis et al., 2012a).

2.8. Immunoassays

The measurement of TGF-β1 and uPA secretion in CM was performed with commercially available immunoassays (Quantikine; R&D Systems), using the manufacturer's instructions. Protein concentrations were calculated via extrapolation from a standard curve, using recombinant proteins as standards.

2.9. Real-time PCR

Quantitative PCR was performed by using 1X SYBR green reagent (Applied Biosystems) and transcript levels of claudin-11 (CLDN11), urokinase-type plasminogen activator (PLAU), tissue inhibitor of metalloproteinase 1 (TIMP1) and integrin-a2 (ITGA2) were measured on a 7500 ABI System. The following 5′-3′ forward (F) and reverse (R) primer sequences were used:

B-actin-F: CACCATTGGCAATGAGCGGTTC, -R: AGGTCTTTGC GGATGTCCACGT CLDN11-F: GGCTGGTGTTTTGCTCATTCTGC, -R: AGCACCAATCCAGCCTGCATAC PLAU-F: GGCTTAACTCCAACACGCAAGG, -R: CCTCCTTGGAACGGATCTTCAG TIMP1-F: GGAGAGTGTCTGCGGATACTTC, -R: GCAGGTAGTGATGTGCAAGA GTC ITGA2-F: TTGCGTGTGGACATCAGTCTGG, -R: GCTGGTAT TTGTCGGACATCTAG.

2.10. Stable isotope labeling with amino acids in cell culture (SILAC)

18Co cells were seeded at low confluence (~25%) in T25 flasks and the cells in each flask were metabolically labeled with either heavy [Arg(+6), Lys(+8)] or light SILAC conditioned media (Dulbecco's Modified Eagle's Medium, 10% dialyzed FBS) for five passages, as previously described (Ong et al., 2002). Labeled 18Co cells were then detached, using a non-enzymatic dissociation buffer, and placed in new T25 flasks in triplicates. Cells were left overnight to adhere and begin proliferation and were subsequently washed twice with PBS, before treated with either previously generated, light-labeled HT29 CM or heavy-labeled 18Co CM, for 48 h. After the termination of the experiment, cells were washed twice with PBS, centrifuged at 1500 *g* for 5 min and supernatants were discarded. Cell pellets were resuspended using 300 μL of 0.1% RapiGest (Waters Inc.) in 25 mmol/L ammonium bicarbonate and sonicated three times for 30 s. The mixtures were centrifuged for 20 min at 15,000 *g*, to remove the remaining debris. Protein samples were then mixed at 1:1 ratio to a total of 250 μg of total protein each (125 μg from HT29-treated and 125 μg from 18Co-treated cells). The three combined replicates were then denaturated in a water bath for 50 min at 80 °C, reduced with 10 nmol/L dithiothreitol (Sigma–Aldrich) for 10 min, at 70 °C, alkylated with 20 nmol/L iodoacetamide (Sigma–Aldrich) for 60 min and were trypsin-digested (Promega) at a ratio of 1:50 (trypsin:protein concentration) for 8 h. The resulting tryptic peptides were reconstituted in 120 μL of 0.26 mol/L formic acid, in 10% acetonitrile. The samples were subjected to strong cation exchange chromatography (SCX) using an Agilent 1100 system, before LC-MS/MS, as previously described (Prassas et al., 2011). Each fraction was run with a 55-min gradient and eluted peptides were subjected to one full mass spectrometry (MS) scan (450–1450 *m/z*) in the Orbitrap at 60,000 resolution, followed by six data-dependent MS/MS scans in the linear ion trap (LTQ Orbitrap). Unassigned charge states and charges +1 and +4 were ignored. RAW files were uploaded into MaxQuant21 version 1.1.1.25 (Cox and Mann, 2008) and searched with the Andromeda22 software against the non-redundant IPI human v.3.71 database as previously described (Cox et al., 2009). Arg(+6) and Lys(+8) were set as heavy labeled with a maximum of three labeled amino acids per peptide. During the search, the IPI human FASTA database was randomized and searched with a false-positive rate of 1% at the peptide and protein levels. Only proteins identified with at least 2-unique peptides were considered for further analysis.

2.11. Statistical analysis

All graphs are presented as mean values with standard deviations calculated from all the experimental and technical replicates. Statistical significance was examined by the Mann–Whitney *U*-test and $p < 0.05$ was considered significant. The statistical software EpiInfo version 7.0.8.0 was used for all analyses.

3. Results

3.1. The colon cancer cell line HT29 induces collective migration of normal colonic fibroblasts

It has been shown that cancer-associated stromal responses may vary in different types of cancer, and in addition,

prognostic outcome has been strongly associated with specific gene and protein expression signatures in the cancer-associated stroma (Finak et al., 2008). This stromal response diversity has been, in part, attributed to the secretion of a wide variety of signals and soluble factors originating from different cancer types and/or subtypes (Bertos and Park, 2011; Finak et al., 2006). Based on these, we hypothesized that CAFs would respond differently to secreted factors originating from cancer cells with diverse genetic backgrounds. To test this hypothesis, we collected CM from three different colon cancer cell lines, HT29, SW480 and SW620 [all with established and diverse genetic backgrounds (Gustafson et al., 1996; Leibovitz et al., 1976; Popanda et al., 2000; Shi et al., 1983)], then, we stimulated normal colonic fibroblast (18Co) monolayers and monitored diverse motogenic reactions inflicted by these CM in cell scratch assay setups (Figure 1A). 18Co cells could utilize both autocrine (18Co CM) and paracrine (HT29/SW480/SW620 CM) growth factors to heal a proportion of the initial wound gap, since the mean wound length (MWL) was bigger in SF-treated (control) compared to all the other experimental conditions (Figures 1A and B). Also, the MWL was significantly smaller in all cancer cell-CM-treated 18Co cells compared to the 18Co-CM-treated ones ($p < 0.05$) (Figure 1B). Further investigations revealed that both SW480-CM- and SW620-CM-treated 18Co cells almost healed the entire wound at 48 h post-stimulation, while the HT29-CM-treated 18Co cells healed approximately 60% of it (Figure 1B). In a complementary fashion to MWL assessment, we performed cell proliferation assays using the same experimental conditions. HT29-CM-, SW480-CM- and SW620-CM-treated 18Co cells had higher proliferation rates compared to both SF- and autocrine-treated 18Co-CM (Figure 1C).

To exclusively demonstrate differences in the migratory behavior of 18Co cells without taking into consideration their proliferation status, we assessed the number of migrating cells per default squared area (NMC/DSA) in the same experimental conditions. A significant increase in NMC/DSA was observed in the SW480-CM- and SW620-CM- ($p < 0.05$), but not in the HT29-CM-treated 18Co cells, when compared to the control conditions (Figure 1D).

Since the previous two metrics demonstrated that HT29 CM could increase the migratory potential of 18Co without prominent presence of individual migratory cells in the wound area (Figure 1B and D), it was tempting to speculate that the HT29-secreted motogenic signals, in contrast to the SW480/SW620 ones, may preferentially cause collective migration in 18Co. Fibroblast collectives or cohorts were assessed according to definition criteria established by Rorth (2009) (Rorth, 2009). To gain further insight into this hypothesis, we assessed a specific parameter of collective cell migration, the invasive growth potential (IGP), using the same experimental conditions (Figure 1E). A mild increase of the IGP was noticed between the cancer cell-CM-treated 18Co cells and the control-CM-treated ones at 24 h (Figure 1E, left graph). However, there was a significant (~4-fold) increase ($p < 0.05$) in the IGP of the HT29-CM-treated NFs compared to the SF control, at 48 h (Figure 1E, right graph). A similar assessment for the SW480-CM- and the SW620-CM-treated 18Co cells was not possible at 48 h, because the wounds had been healed in these conditions at an earlier time-point (Figure 1A).

We finally assessed the impact of cancer cell secreted factors on direction-sensing, by investigating the protrusion activity and the formation of front-to-rear axis towards the 120° angle facing the wound (Figure 1E, enlarged illustrations), as previously described (Etienne-Manneville, 2008). Such measurements revealed that 18Co cells treated with SF medium had random direction-sensing (~31%), while cells treated with either autocrine or paracrine factors had a significantly increased ($p < 0.05$) ability for polarization with direction-sensing (Figure 1F, right graph). Moreover, HT29-specific factors could cause an increased ($p < 0.05$) protrusion activity of 18Co cells towards the wound gap, when compared with the autocrine stimulation (Figure 1F, right graph).

From these data, it is evident that 18Co cells obtain dissimilar motogenic responses upon stimulation with various colon cancer cell CM. In contrast to SW480/SW620, the genetic background of the HT29 cells might support the secretion of factors, which contribute to the collective behavior of CAF migration.

3.2. *Proteomic analysis of HT29-CM-stimulated normal colonic fibroblasts reveals upregulation of prominent markers of fibroblast-to-myofibroblast differentiation*

Next, we sought to identify responsible mediator(s) for the collectivity of 18Co migration, as seen in the HT29-dependent setup of the experiments in Figure 1. For this reason, we proceeded to gain global overview of protein perturbations seen in 18Co cells, upon HT29 CM stimulation, using a quantitative proteomic approach (SILAC) coupled to mass spectrometry (MS/MS), as previously described (Prassas et al., 2011).

In our experimental setup (Figure 2A), heavy-labeled 18Co cells were stimulated with the autocrine medium (18Co SILAC CM) which served as the “control pool”, while light-labeled 18Co cells were stimulated with cancer medium (HT29 SILAC CM) which served as the “stimulation pool”. Theoretically, stimulation with either HT29 or 18Co CM would disturb the efficient labeling of the experimental cells with heavy or light amino acids. For this reason, the stimulation media used in the SILAC approach were also appropriately labeled. Specifically, 18Co SILAC CM was generated from heavy labeled 18Co cells, cultured independently. Concordantly the HT29 SILAC CM was generated from light-labeled HT29 cells, also cultured independently for a total of 5 passages (Figure 2A). After the termination of stimulations, cells were harvested and protein samples were mixed in 1:1 heavy:light ratio before MS analysis. Protein quantification was based on the differential intensities of the peaks of the precursor ions of heavy versus light peptides (Figure 2A). In total, we have been able to quantify 2326 proteins (Supplementary Table 1). The mean distribution of HT29-CM-induced protein alterations is shown in Figure 2B. As expected, the vast majority of proteins were found with a <2-fold up- or downregulation (Figure 2B). It should be noted that since the HT29-CM-stimulated condition corresponds to the light labeling, all proteins that were found with a heavy:light ratio of less than 0.5 were >2-fold upregulated, whereas all proteins that were found with a heavy:light ratio of more than 2, were >2-fold downregulated. All these differences were statistically significant ($p < 0.05$). Thus, we focused our interest on 25 proteins, which were

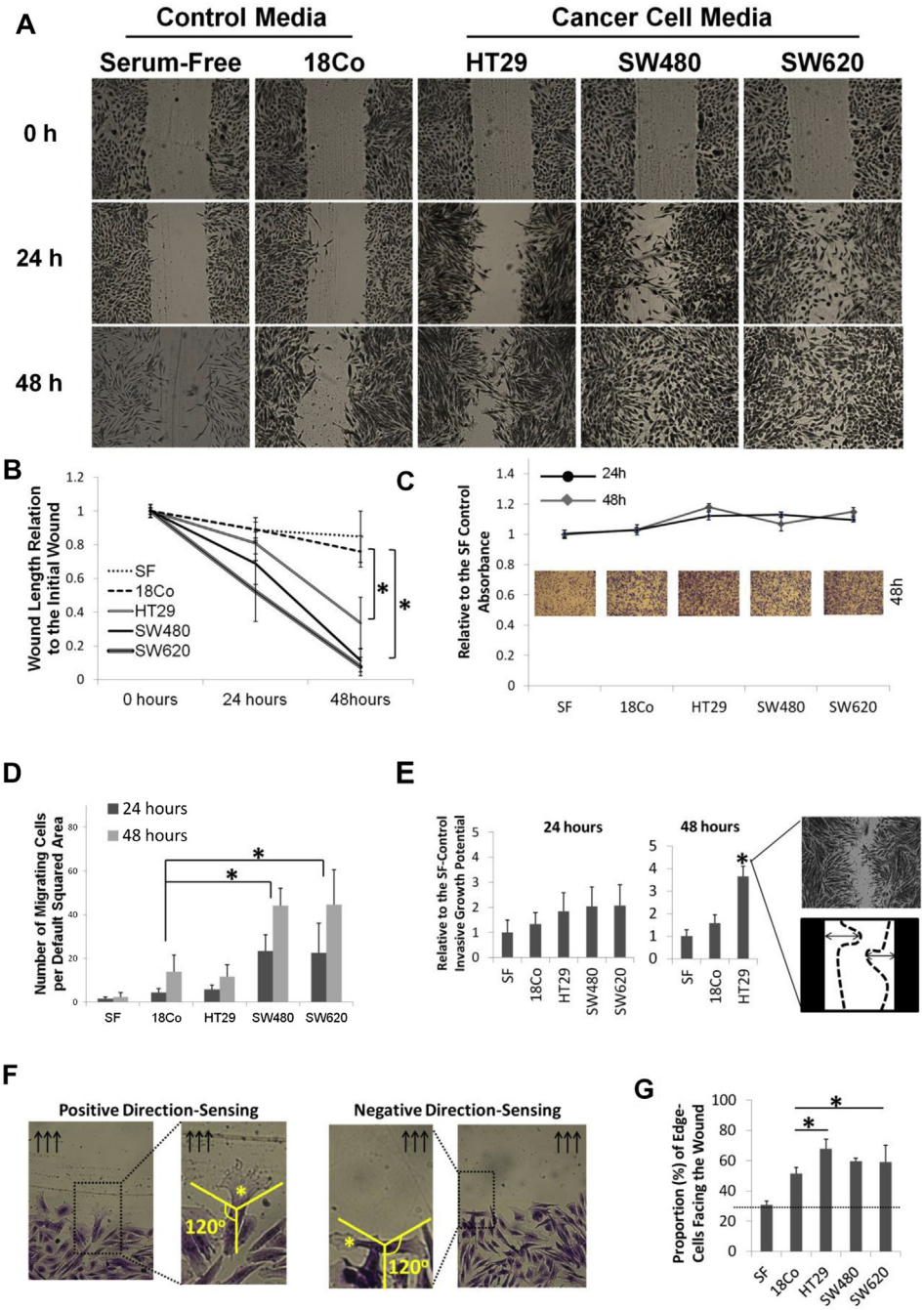

Figure 1 – The colon cancer cell line HT29 induces collective migration of normal colonic fibroblasts. (A) Representative snapshots from the scratch assay; 18Co fibroblasts were treated with various cancer cell line CM and control media and various parameters were measured in a time-dependent manner. (B) MWL assessment; the graph represents the relative closure of the wound to the initial wound gap. *denotes statistical significance ($p < 0.05$, Mann–Whitney U-test). (C) Cell proliferation assay (crystal violet); the graph represents the relative absorbance to the SF-treated condition; figures underneath depict cell confluence in each condition as evaluated through light microscopy. (D) NMC/DSA assessment; the graph depicts the mean number of migrating cells from multiple squared areas, in a time-dependent manner. *denotes statistical significance ($p < 0.05$, Mann–Whitney U-test). (E) IGP assessment; the graph depicts the relative to the SF control IGP of all the CM-treated experimental conditions; the adjacent illustration presents the high IGP observed in the HT29-treated condition. *denotes statistical significance ($p < 0.05$, Mann–Whitney U-test). (F–G) Positive direction sensing assessment (F) at 8h post-scratching; enlarged figures depict fibroblasts that are polarized [cytoplasmic protrusions facing the wound (left panels)] or non-polarized [cytoplasmic protrusions facing a different angle away from the wound (right panels)]; the adjacent graph (G) depicts percentage of the positive cell population facing the wound in each experimental condition; dashed line reveals the 33% cut-off which could be attributed to a random direction-sensing, since the Y method is used. *denotes statistical significance ($p < 0.05$, Mann–Whitney U-test). See also list of abbreviations.

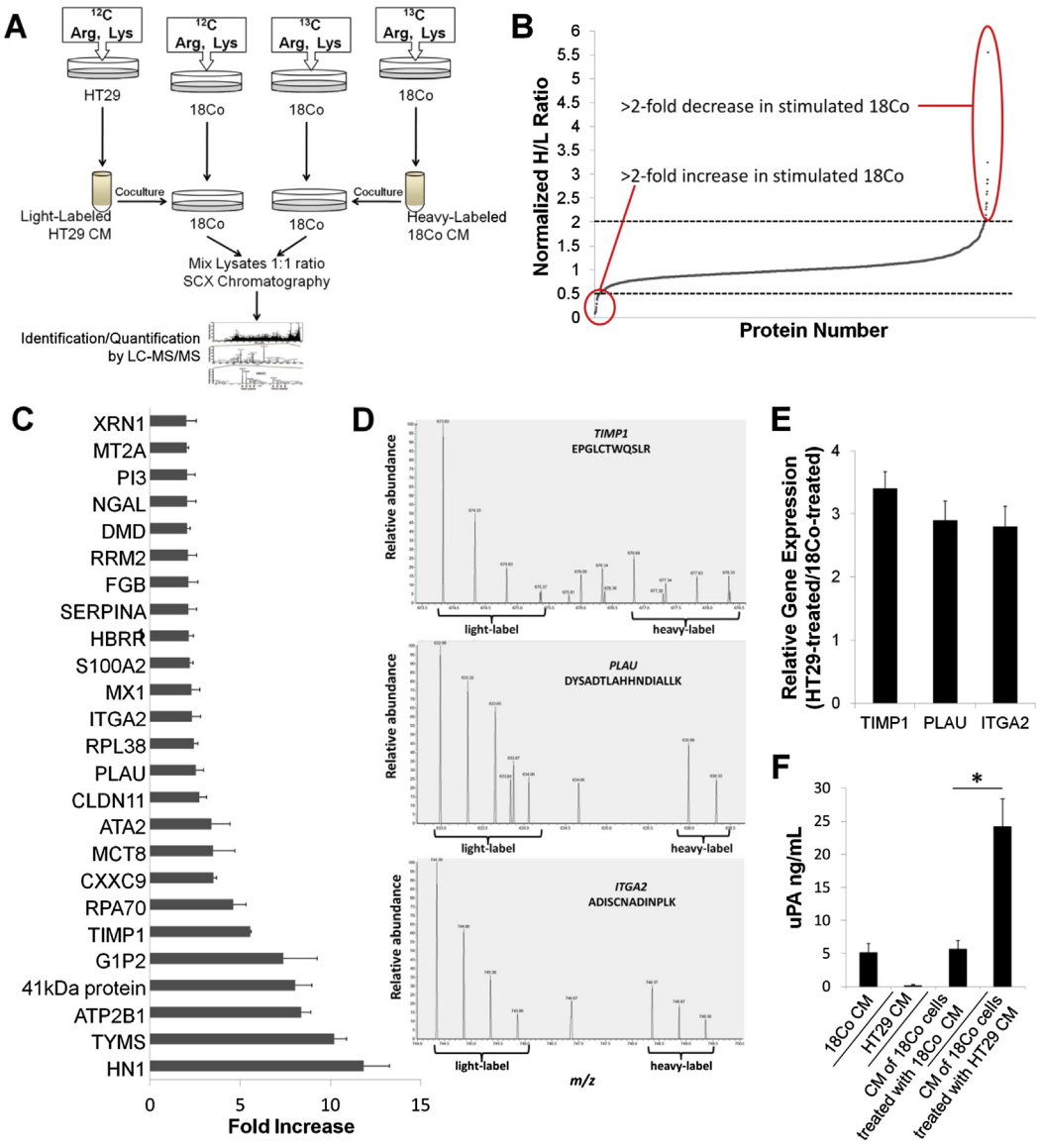

Figure 2 – Quantitative proteomic analysis (SILAC) shows the HT29-recruited CAFs overexpress the tight junction protein, CLDN11. (A) Graphical illustration of metabolic labeling and proteomic pipeline strategies; stimulation of fibroblasts with either 18Co or HT29 medium is performed with CM that have been generated from metabolically labeled 18Co or HT29 cells, respectively. (B) Distribution of all proteins identified plotted against their normalized heavy/light (H/L) ratios (mean ratios from combination of three biological replicates). (C) Proteins presenting with a statistically significant *($p < 0.05$, Mann–Whitney U-test)* >2-fold increase in the HT29-treated 18Co cells were considered for further analysis, resulting in the 25-protein list. (D) MS spectra of representative peptides from markers of myofibroblastic differentiation, showing a statistically significant differential expression between the two experimental conditions. (E) Relative gene expression levels of the three markers of myofibroblastic differentiation, showing a statistically significant differential expression between the two experimental conditions. (F) uPA ELISA; uPA levels were measured in CM derived from the 18C0-CM or HT29-CM stimulated 18Co cells. Basal levels of uPA in 18Co and HT29 CM were also measured. uPA secretion increased in HT29-CM-treated cells compared to the control cells, and this increase did not occur due to uPA presence in the HT29 CM. *denotes statistical significance ($p < 0.05$, Mann–Whitney U-test). See also list of abbreviations.

presented with a statistically significant ($p < 0.05$) >2-fold upregulation (Figure 2C), since these candidates could serve as potential mediators of 18Co collective migration in the HT29-CM-stimulated state.

Of particular interest in this 25-protein dataset was the upregulation of urokinase-type plasminogen activator (PLAU; uPA) in HT29-CM-stimulated 18Co cells, compared to the placebo-treated ones (Figure 2C and D). uPA is an extracellular protease secreted by stromal cells, principally fibroblasts, and its secretion is enhanced upon transdifferentiation of normal fibroblasts into CAFs. Along with matrix metalloproteinases-2 and -9 (MMP2 and MMP9), uPA currently serves as one of the most prominent extracellular protease markers of myofibroblastic differentiation (Kunz-Schughart and Knuechel, 2002) and is particularly expressed in peritumoral stroma at the invasive margins of most desmoplastic

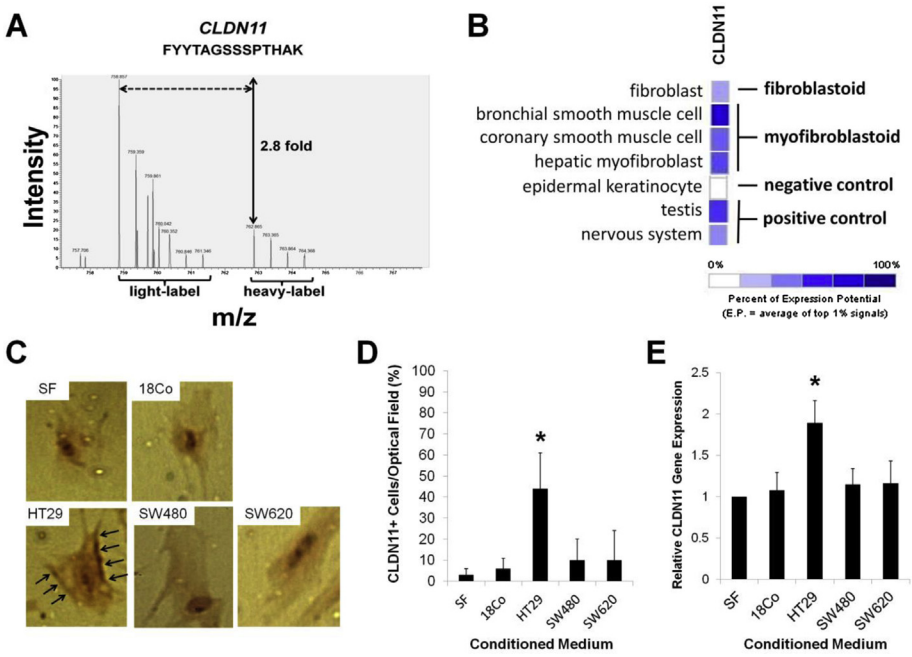

Figure 3 – Validation of HT29-dependent CLDN11 overexpression in 18Co cells. (A) MS spectra of representative peptide from Claudin-11 (CLDN11) showing 2.8-fold differential expression between the two experimental conditions. (B) Gene expression meta-analysis using Genevestigator; the color scale demonstrates the normalized relative differential expression of CLDN11 in a variety of normal arrays. (C) CLDN11 immunocytochemistry (ICC); only HT29-CM-stimulated 18Co cells were able to express CLDN11 (black arrows), preferentially in the membrane of the cells. *Magnifications x100* (D) Quantification of the results obtained in experiment shown in panel (C); graphs represent percentage of positive cells per optical field. **denotes statistical significance ($p < 0.05$, Mann–Whitney U-test).* (E) Relative gene expression levels of CLDN11 in 18Co cells under the same experimental conditions of panel (C); the results verify quantification data of this experiment. CLDN11 is overexpressed only in the HT29-CM-stimulated 18Co cells. **denotes statistical significance ($p < 0.05$, Mann–Whitney U-test).*

cancers (De Wever et al., 2008a). In this 25-protein dataset, integrin-a2 (ITGA2) represents another protein that could be highly associated with fibroblast-to-myofibroblast differentiation (Figure 2C and D). It is now postulated that CAFs shift their focal adhesion apparatus, towards loosening the stiff anchoring of their integrins to components of ECM (Brenmoehl et al., 2009; Dey et al., 2011). Among the plethora of focal adhesion mediators, the overexpression of ITGA2 in lung cancer CAFs compared to normal lung fibroblasts had been determined, in a tissue-wide microarray analysis (Navab et al., 2011). Finally, the 25-protein dataset revealed upregulation of the tissue inhibitor of metalloproteinase-1 (TIMP1) (Figure 2C and D), a prominent marker of CAFs (Zanotti et al., 2010), participating in ECM remodeling and proteolytic cascades at the cancer invasion front (Clavel et al., 1992). To further substantiate the overexpression of these CAF markers in the SILAC experiment, we confirmed significantly increased mRNA levels of uPA, ITGA2 and TIMP1 in HT29-CM-treated 18Co cells, using real-time PCR (Figure 2E). For further verification, we investigated uPA secretion in the CM of HT29-CM-treated and non-treated 18Co cells, using an uPA-specific immunoassay. We found that uPA levels were significantly increased in the HT29-CM-treated 18Co cells, when compared to the 18Co-CM-treated ones (Figure 2F).

The re-discovery of prominent markers of myofibroblastic differentiation in the 25-protein dataset provides further accuracy to our quantitative proteomic approach. Thus, SILAC analysis suggests that 18Co cells could be transformed into CAFs upon stimulation with soluble factors originating from the HT29 genetic background.

3.3. *HT29-recruited CAFs overexpress the tight junction protein, claudin-11 (CLDN11)*

Of all the candidates of the 25-protein dataset, we selected claudin-11 (CLDN11) as the most promising mediator of 18Co collective migration, for the following reasons. First, CLDN11 belongs to the family of claudins, a group of cell adhesion molecules, which participate in the formation of cell-to-cell tight junctions, further regulating paracellular permeability and epithelial polarization (Tsukita and Furuse, 1999, 2002). Second, tight junctions are hallmarks of epithelial cells and they tend to be lost in mesenchymal cells or in cases where epithelial cells undergo epithelial-to-mesenchymal transition (De Wever et al., 2008b; Kalluri and Weinberg, 2009). Third, CLDN11 was found to be approximately 2.7-fold overexpressed in the HT29-CM-stimulated 18Co cells, however, this overexpression was highly reproducible among all three replicates (Figure 3A).

Before further analysis, we sought to validate our SILAC data through both bioinformatic and experimental means. For the former, we took advantage of the Genevestigator database and performed gene expression meta-analysis in a large cohort of tissue microarray experiments, to investigate the

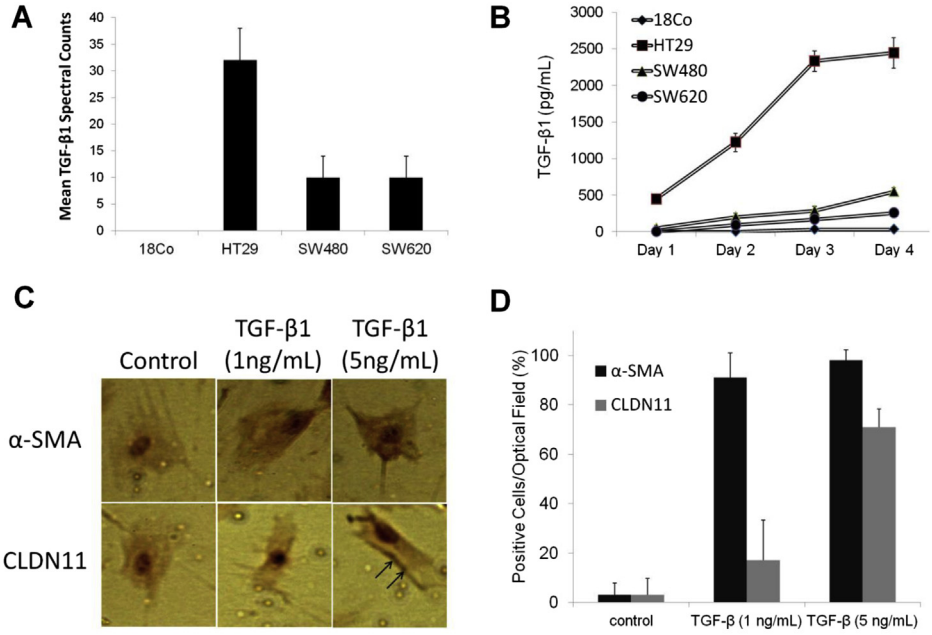

Figure 4 – Association of CLDN11 overexpression in 18Co cells with TGF-β1. (A) Mean TGF-β1 spectral counts after normalization from proteomic datasets obtained from previous work by our group (Karagiannis et al., 2012a). (B) TGF-β1 ELISA; TGF-β1 levels were measured in CM derived from the respective cell lines. TGF-β1 secretion increased in HT29 CM in a time-dependent manner, while it remained at basal levels for SW480, SW620 and 18Co cells. Such observations are in concordance with the proteomic data shown in panel (A). (C) CLDN11 and α-SMA ICC; 18Co cells were stimulated with TGF-β1 in a dose-dependent manner and expression of CLDN11 and α-SMA was evaluated. Note that cytoplasmic α-SMA expression increased even at 1 ng/ml TGF-β, but CLDN11 membranous expression (black arrows) is found at higher levels of TGF-β1 (5 ng/ml). (D) Quantification of the results obtained in experiment shown in panel (D); graphs represent percentage of positive cells per optical field. *Magnifications x100*.

tissue specificity of CLDN11. This analysis demonstrated the specific expression of CLDN11 in the normal testis and nerve myelin sheaths (Figure 3B), an observation that served as a positive control for the meta-analysis, since it is well documented that these are the specific sites where CLDN11 expression and function are encountered (Mazaud-Guittot et al., 2010; Morita et al., 1999; Tiwari-Woodruff et al., 2001). In addition, this meta-analysis demonstrated that CLDN11 is not expressed in the remaining epithelial tissues (Figure 3B), as various members of this family are (Tsukita and Furuse, 2002), and consequently, these epithelial arrays served as negative controls for the meta-analysis (Figure 3B). Thus, we compared the expression of CLDN11 in multiple arrays of tissues/cells that retain the myofibroblastic phenotype (i.e. bronchial and coronary smooth muscle cell arrays, as well as hepatic myofibroblast arrays), with its relative expression to pure fibroblastic arrays and found that CLDN11 was significantly increased in all of the "myofibroblastoid" arrays compared to the "fibroblastoid" ones (Figure 3B).

For the experimental validation, we restimulated 18Co cells with the same conditions of experiments shown in Figure 1, and examined the expression of CLDN11 with immunocytochemistry (ICC). In this case, HT29-CM-stimulated 18Co cells showed strong immunoreactivity for CLDN11, which was almost exclusively localized on cell membranes (Figure 3C, black arrows). Interestingly, approximately 45% of the 18Co cell population was found positive for CLDN11, a proportion that was significantly higher than the remaining conditions (Figure 3D). Specifically, less than 10% of the population was found CLDN11 positive in the SF Control-CM-, 18Co-CM, SW480-CM- and SW620-CM-stimulated 18Co cells (Figure 3D). These quantitative data were also confirmed at the mRNA level (Figure 3E).

Along with the SILAC data in the previous section, the data in this section indicate that increased expression of CLDN11 follows the transition of normal fibroblasts into CAFs and in addition, this transition is strongly-dependent in specific cancer cell genetic backgrounds (HT29 over SW480/SW620).

3.4. *CLDN11-overexpression in colonic CAFs is TGF-β-dependent*

Given the above, we reasoned that the HT29 background, in contrast to the SW480/SW620 ones, might hold unique microenvironmental motogens, responsible for the increased expression of CLDN11 and subsequent cohort configuration in CAFs. Currently, TGF-β is the major growth factor that is known to act as a chemotactic agent for CAFs and promote fibroblast-to-myofibroblast transdifferentiation (Ronnov-Jessen and Petersen, 1993).

Thus, we reasoned that the major difference between the HT29 and SW480/SW620 genetic backgrounds could be the differential secretion of TGF-β. To examine this possibility, we deployed both proteomic and biochemical means. For the

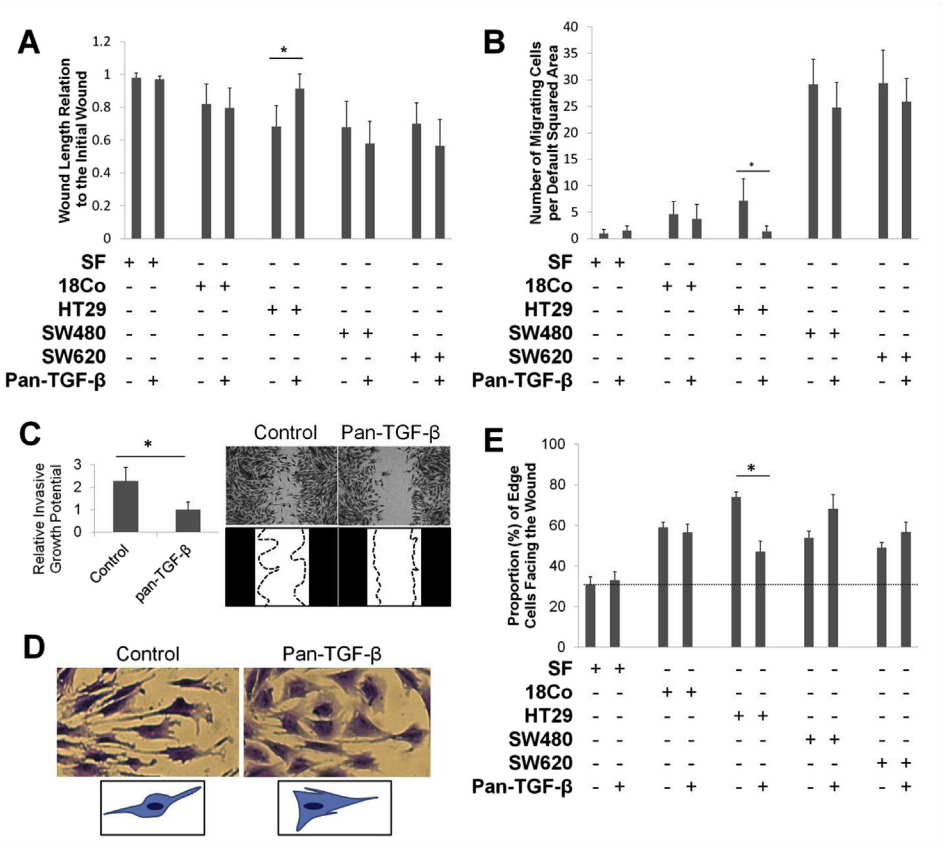

Figure 5 – Endogenous TGF-β1, secreted by HT29 cells, induces collective configuration during CAF migration. (A) MWL assessment; the graph represents the relative closure of the wound to the initial wound gap. *denotes statistical significance ($p < 0.05$, Mann–Whitney U-test). (B) NMC/DSA assessment; the graph depicts the mean number of migrating cells from multiple squared areas, in a time-dependent manner. *denotes statistical significance ($p < 0.05$, Mann–Whitney U-test). (C) IGP assessment; the graph depicts reduction of IGP in the PanTGF-β1/HT29-CM-stimulated compared to HT29-CM-stimulated 18Co cells; the adjacent illustration presents a representative snapshot. *denotes statistical significance ($p < 0.05$, Mann–Whitney U-test). (D) Cell morphology is altered from a more mesenchymal/elongated shape to a more spindle/polyhedron-like shape, upon treatment with the pan-TGF-β neutralizing antibody. (E) Positive direction sensing assessment; note, that only the HT29-CM-treated cells are affected by the use of the neutralizing antibody. *denotes statistical significance ($p < 0.05$, Mann–Whitney U-test). Figures A-D, 48h post-stimulation; Figure E, 8h post-stimulation.

former, we took advantage of comprehensive protein datasets obtained from our previous study (Karagiannis et al., 2012a). In that study (Karagiannis et al., 2012a), we had performed proteomic analysis of CM (termed "secretome analysis") of various colon cancer and colonic fibroblast cell lines, including SW480/SW620, HT29 and 18Co. Spectral counts were normalized in all these secretome datasets, using a well-accepted method (Collier et al., 2010), to allow for direct quantitative comparison of specific secreted proteins. Here, we compared TGF-β1 spectral counts in all the secretome datasets and found that secretion of TGF-β1 was at least three times higher in HT29 cells compared to SW480 or SW620 cells, while no TGF-β1 was secreted by 18Co cells (Figure 4A).

For the biochemical validation, we utilized a specific TGF-β1 immunoassay and measured TGF-β1 levels in the CM of all these cell lines in a time-dependent fashion. In general, TGF-β1 secretion was increased over time in all cell lines, but it consistently remained higher in the HT29 cell line compared to all the other genetic backgrounds (Figure 4B). At 2 days post-seeding, the time-point when stimulation media of the experiments in Figures 1 and 2 were collected, the observed TGF-β1 secretion was more than approximately 1.5 ng/mL for HT29 cells, whereas it was significantly less, or even absent, for the rest of the genetic backgrounds (SW480/SW620, 18Co) tested (Figure 4B).

The differential secretion of TGF-β1 could potentially explain the differential migratory pattern, as well as the expression of CLDN11 in HT29-CM-stimulated 18Co cells. To further demonstrate that TGF-β1 was the responsible cytokine for these effects in our experimental setups, we investigated the effect of exogenous TGF-β1 in fibroblast-to-myofibroblast transdifferentiation and CLDN11 expression in 18Co cells. Specifically, 18Co fibroblasts were stimulated with increasing doses of TGF-β1, and then, α-SMA or CLDN11 expression were evaluated by ICC. TGF-β1 stimulation caused a dose-dependent increase in cytoplasmic α-SMA and membranous CLDN11 expression in 18Co cells (Figure 4C). In particular, even 1 ng/mL TGF-β1 was sufficient to cause an almost 100% induction of α-SMA positive 18Co cells (Figure 4D), an observation consistent with the literature (Brenmoehl et al., 2009;

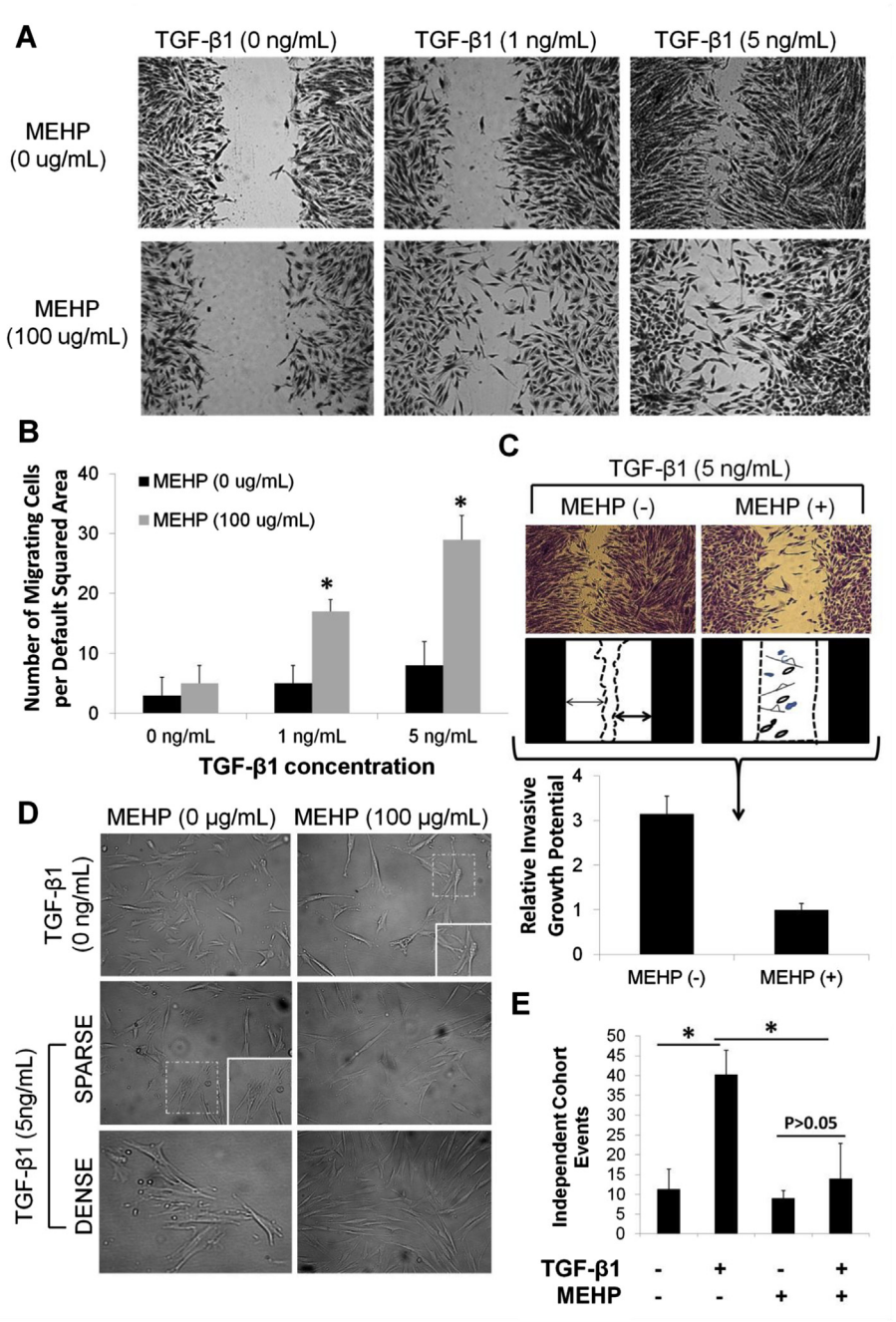

Figure 6 – MEHP-dependent disruption of tight junction protein CLDN11 attenuates the TGF-β1-dependent collective configuration during CAF migration. (A) Representative snapshots from the scratch assay; 18Co fibroblasts were treated with TGF-β1 in a dose-dependent manner, with or without MEHP (100 μg/mL) and various parameters were measured. (B) NMC/DSA assessment; the graph depicts the mean number of migrating cells from multiple squared areas, in a dose-dependent manner. **denotes statistical significance ($p < 0.05$, Mann–Whitney U-test)*. (C) IGP assessment; the graph depicts reduction of IGP in the MEHP/TGF-β1-stimulated compared to TGF-β1-stimulated 18Co cells; the adjacent figure/illustration presents a representative snapshot. **denotes statistical significance ($p < 0.05$, Mann–Whitney U-test)*. (D) Investigation of cohort formation in non-confluent 18Co monolayers treated with TGF-β1 in a dose-dependent manner with or without MEHP (100 μg/mL). *Magnifications x40 (inlet magnification X65)*. (E) Quantification of the results obtained on experiment shown in (D); graphs represent number of CAF cohorts as measured by three blinded observers. *See also list of abbreviations*.

Denys et al., 2008; Desmouliere et al., 1993; Hawinkels et al., 2009; Lewis et al., 2004). However, more than 20% of 18Co cells had CLDN11-positive cell membranes at 1 ng/mL TGF-β1, while approximately 70% of 18Co cells were CLDN11-positive at 5 ng/mL of TGF-β1 (Figure 4D).

Consistent with the above, data from Figure 3D further demonstrate that treatment of 18Co cells with 2-day HT29 CM is able to induce ~45% CLDN11 immunoreactivity. Given that the TGF-β immunoassay (Figure 4B) showed that HT29 cells secrete approximately 1.5 ng/mL of TGF-β on day 2

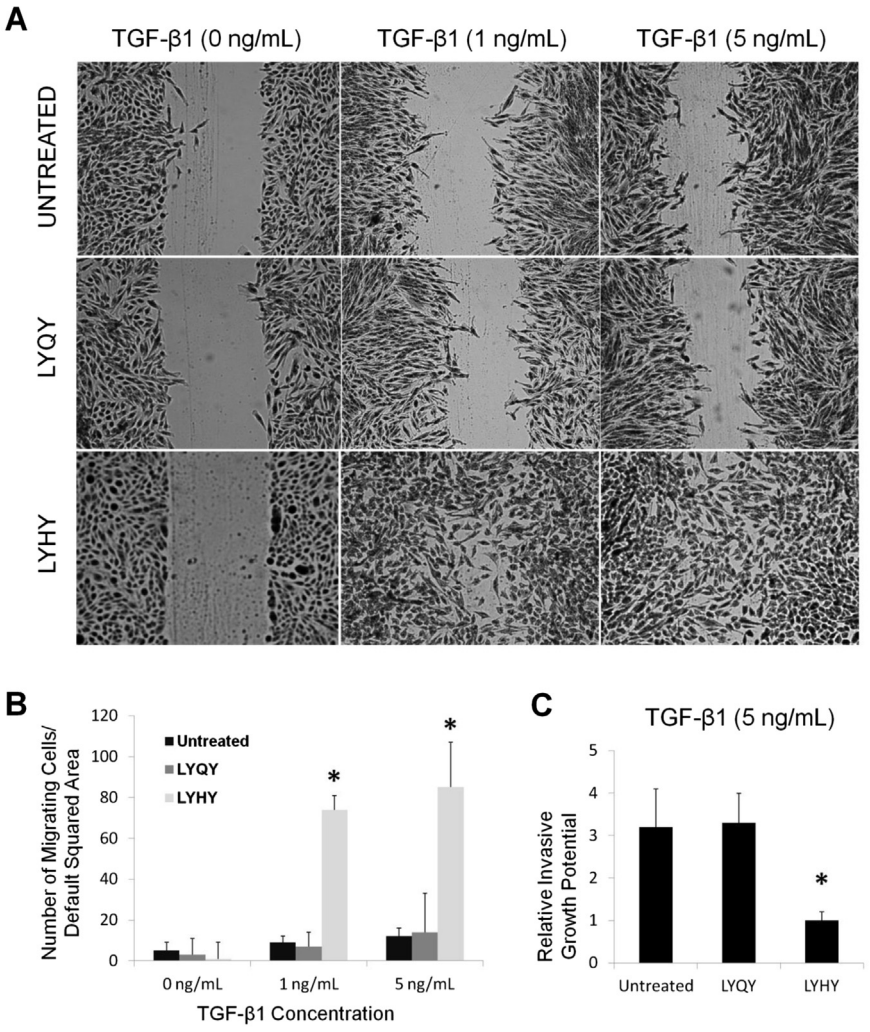

Figure 7 – LYHY-dependent disruption of OCLN attenuates the TGF-β1-dependent collective configuration during CAF migration. (A) Representative snapshots from the scratch assay; 18Co fibroblasts were treated with TGF-β1 in a dose-dependent manner, and either left untreated or treated with the active (LYHY; 350 μM) or control peptide (LYQY; 350 μM) for 48 h and NMC/DSA and IGP were measured. (B) NMC/DSA assessment; the graph depicts the mean number of migrating cells from multiple squared areas, in a dose-dependent manner. **denotes statistical significance ($p < 0.05$, Mann–Whitney U-test)*. (C) IGP assessment; the graph depicts reduction of IGP in the LYHY/TGF-β1-stimulated compared to LYQY/TGF-β1-stimulated or TGF-β1-stimulated 18Co cells. **denotes statistical significance ($p < 0.05$, Mann–Whitney U-test). See also list of abbreviations*.

post-seeding, we conclude that TGF-β1 is sufficient but not necessary in causing CLDN11 overexpression in 18Co cells. Since other factors may be involved in this process secreted factors of the HT29 CM should be further explored in the future.

Thus, observations from this section suggest that CLDN11 overexpression is associated with TGF-β1-dependent fibroblast-to myofibroblast transdifferentiation in 18Co cells."

3.5. *HT29-secreted TGF-β1 induces collective configuration in CAFs*

Further, we wished to test whether the endogenous TGF-β was specifically responsible for the induction of collective configuration in HT29-CM-stimulated 18Co cells. To test this, we repeated the migration assays of Figure 1, additionally utilizing a pan-TGF-β neutralizing antibody. Based on our findings so far, we expected that the neutralizing antibody would alleviate the collective nature of 18Co migration in the HT29-CM-stimulated 18Co cells, due to reduction of bioavailable active TGF-β in the CM. Indeed, pan-TGF-β significantly delayed the closure of the *in-vitro* wound (MWL assessment) in the HT29-CM-stimulated 18Co cells, while other conditions remained unaltered (Figure 5A). Moreover, pan-TGF-β slightly reduced the NMC/DSA in the HT29-CM-stimulated 18Co cells, while the remaining conditions remained unaltered (Figure 5B). Overall, there was an approximately 2.5-fold abrogation of IGP with the parallel utilization of pan-TGF-β neutralizing antibody in HT29-CM-stimulated 18Co cells (Figure 5C). In addition, we noticed that the utilization of the pan-TGF-β neutralizing antibody induced less fibroblastic/mesenchymal phenotype in HT29-CM-stimulated 18Co cells

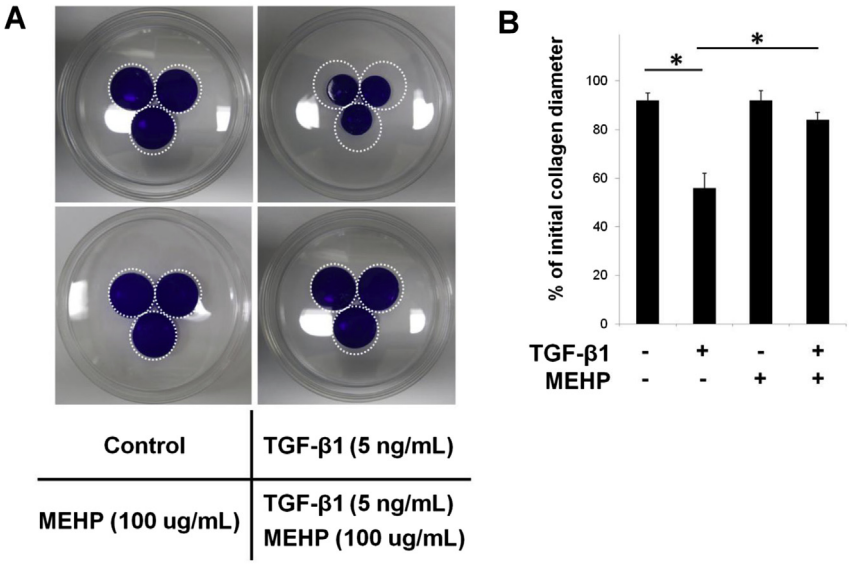

Figure 8 – TGF-β1 enhances the CLDN-11-dependent contractile ability of CAFs (A) Collagen gels containing 18Co cells in triplicates were left untreated or stimulated with either TGF-β1, or MEHP or both, for 24 h. The circle with dashed white line corresponds to the diameter of the respective control gel at 0 h. (B) Quantification of the previous experiment, demonstrating the length of collagen gel diameter of the experimental condition relatively to the initial diameter; the value is indicated as percentage of the relative reduction. **denotes statistical significance ($p < 0.05$, Mann–Whitney U-test).*

(Figure 5D). Moreover, the utilization of the pan-TGF-β neutralizing antibody significantly ($p < 0.05$) attenuated the ability of the edge cells for polarization in the HT29-stimulated condition, whereas the ability for positive direction-sensing was unchanged in all other experimental conditions (Figure 5E). These data suggest that: (a) the altered migratory behavior of 18Co cells by the HT29 genetic background is dependent on the endogenous secretion of TGF-β by HT29 cancer cells (Figure 5A–C), (b) the endogenously-secreted TGF-β might preserve migratory phenotype in CAFs (Figure 5D) and (c) TGF-β signaling could be responsible for polarized migration of CAFs (Figure 5E).

Subsequently, we generated scratches in confluent 18Co monolayers and stimulated them with increasing doses of exogenous TGF-β (Figure 6A). TGF-β1 stimulation was followed by non significant increase in the NMC/DSA (Figure 6A–B) and 18Co cells migrated in a collective configuration (Figure 6A), validating all combined results in Figures 1 and 5. Interestingly, the utilization of the tight junction disruptor MEHP, which is known to transcriptionally downregulate Claudin-11 and Occludin (Chiba et al., 2011), abrogated this effect and caused an increase of NMC/DSA in both the 1 ng/mL and 5 ng/mL TGF-β1-stimulated 18Co monolayers (Figure 6A–B). Additionally, 18Co cells that were stimulated with 5 ng/mL TGF-β1 exerted an approximately 3-fold higher IGP, when compared to the same cells treated with both 5 ng/mL TGF-β1 and 100 μg/mL of MEHP (Figure 6C).

We additionally demonstrated these conclusions, using similar experimental setups in non-confluent 18Co monolayers. We evaluated the ability of 18Co cells to grow in collective configuration by measuring "independent cohort events", assessed by three blinded observers. In the TGF-β-negative condition, the stimulation of 18Co cells with 100 ug/mL MEHP affected neither the morphology of the cells (Figure 6D) nor the mean number of independent cohort events (Figure 6E). Interestingly, 18Co cells were able to form cell-to-cell adhesions to some extent (Figure 6D), however, cells were not polarized towards the same axis and thus, such cell-to-cell adhesions were not considered as independent cohort events. As soon as 18Co cells were stimulated with 5 ng/mL TGF-β1, independent cohort events were evident in both the low- and high-confluence conditions (Figure 5D). Therefore, there was a statistically significant ($p < 0.05$) increase in the mean number of independent cohort events, between TGF-β1 stimulated and non-stimulated conditions (Figure 6E). Interestingly, in the TGF-β-positive condition, the stimulation of 18Co cells with 100 ug/mL MEHP significantly reduced the mean number of independent cohort events (Figure 6E). Interestingly, in the high-confluence conditions, 18Co cells did not appear to come in physical contact, thus being negative for cell-to-cell adhesions, despite growing in very high density (Figure 6D).

3.6. TGF-β1-dependent collective migration of CAFs is occludin (OCLN)-dependent

The next question was whether disruption of tight junctions by another means would produce a similar result. We utilized a peptide previously reported to disrupt tight junctions (Beeman et al., 2009; Blaschuk et al., 2002). This peptide contained the LYHY sequence from the second extracellular loop of mouse occludin circularized for stability by oxidation of flanking cysteine residues. Confluent 18Co fibroblast monolayers, similar to the scratch assay setups of Figure 6A, were prepared and a dose-dependent gradient of TGF-β1 was applied in the wells (0, 1 and 5 ng/mL). Then, the wells were

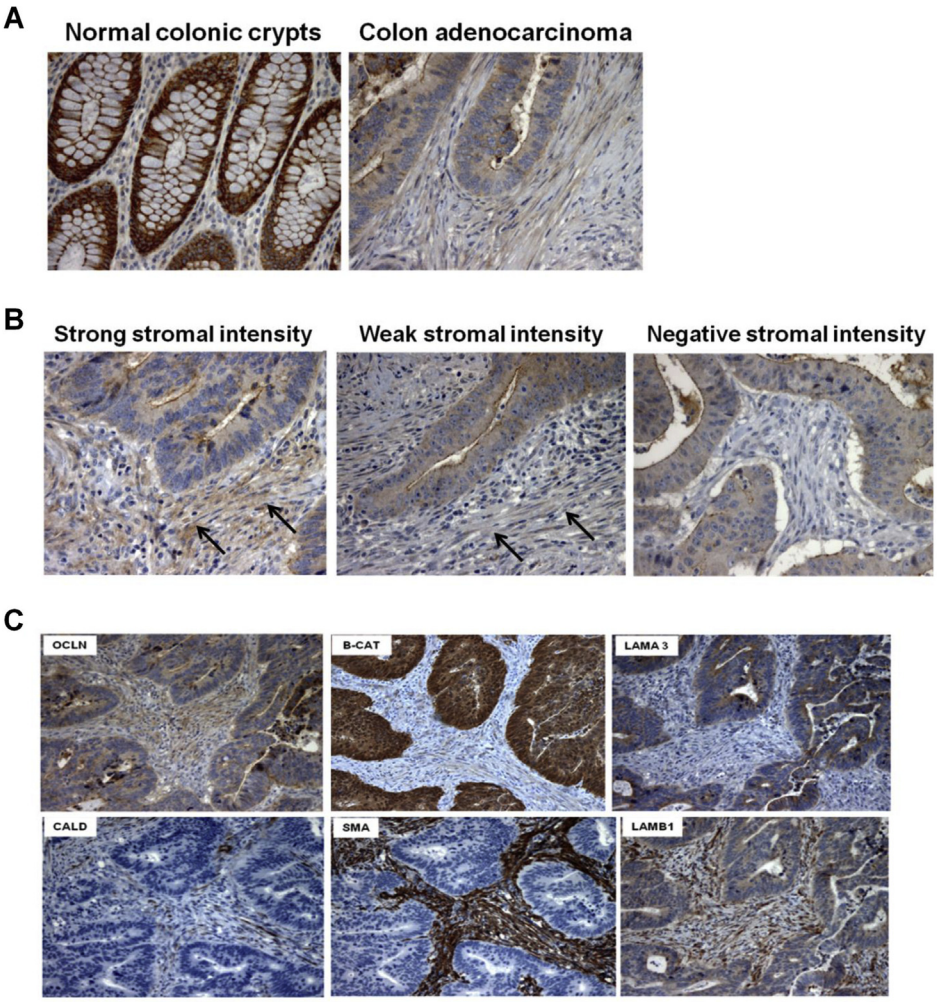

Figure 9 – CAF cohorts express the tight junction protein occludin, but not claudin-11, in desmoplastic lesions of colorectal cancer patients. (A) Occludin (OCLN) IHC; note the strong membranous expression of OCLN in normal colonic crypts, representing tight junctions; OCLN expression is substantially reduced in the adenocarcinoma from the same patient. *Magnification x200* (B) Variable expression of OCLN expression by CAFs; arrows depict OCLN + stromal cells. *Magnification x200* (C) Characterization of the OCLN + stromal subpopulation with respect to co-expression of other proteins including: B-CAT, beta-catenin; LAMA3, laminin-alpha3; LAMB1, laminin-beta1; CALD, h-caldesmon; SMA, smooth muscle actin. *Magnification x100*.

either left untreated or treated with the LYHY or the control (i.e. LYQY) peptide (350 μM) for 48 h (Figure 7A). Control peptide-treated and untreated 18Co cells presented similar behavior that is collectivity in the TGF-β1-dependent migration (Figure 7A), with significantly lower NMC/DSA (Figure 7B) and significantly higher IGP (Figure 7C), compared to the LYHY-treated 18Co fibroblasts. Thus, disruption of occludin by LYHY alleviates the collective migration of TGF-β1-stimulated CAFs *in vitro*. It should be noted that treatment of 18Co fibroblasts with either of the peptides alone does not affect OCLN and/or CLDN11 mRNA expression levels (data not shown).

Taken together, the data from experiments shown in Figures 5, 6 and 7 indicate that TGF-β is directly responsible for the collective and polarized nature of CAF migration. Consistently, our working hypothesis states that a number of colorectal carcinomas, whose genetic background supports aberrant secretion of TGF-β, could be potentially responsible for recruiting CAF collectives in the peritumoral tumor-host cell interface area.

3.7. *TGF-β1-dependent formation of tight junctions enhances the contractile ability of CAFs*

CAFs are characterized by their enhanced contractile activity, which can be induced by TGF-β and other cytokines such as PDGF and IL-1a (Tingstrom et al., 1992). Tissue contraction mediated by CAFs is considered as the most important cause of increased interstitial pressure, which delays drug delivery to cancer tissues (Heldin et al., 2004). Therefore, we wished to investigate whether the TGF-β1-dependent tight junction formation was responsible, at least in part, for such observed functions of CAFs. To address this issue, collagen contraction assays were performed. The stimulation of 18Co cells with 5 ng/mL TGF-β1 clearly enhanced their ability to cause collagen contraction compared to the control fibroblasts

(Figure 8A). In particular, the stimulated fibroblasts were able to reduce the initial collagen gel diameter by 50%, whereas the control-treated fibroblasts by only 10% (Figure 8B). Further experiments were performed in the presence or absence of the tight junction disruptor MEHP. The addition of the tight junction disruptor MEHP did not affect the ability of the normal fibroblasts to cause collagen gel contraction (Figure 8A–B). On the contrary, addition of MEHP in the concentration of 100 ug/mL was sufficient in completely alleviating the collagen gel contraction induced by 5 ng/mL of TGF-β1 (Figure 8A–B).

The collagen gel contraction experiments presented above suggest that TGF-β1-recruited colonic CAFs exert their functional activities (i.e. collagen contraction) *in vitro*, in a tight junction-dependent manner.

3.8. *CAFs express the tight junction protein occludin (OCLN) in desmoplastic lesions of colorectal cancer patients*

Tight junctions consist of the transmembrane proteins occludin (*Ocln*), one member of the claudin family of proteins (*Cldn1-24*) and other tight junction-associated proteins, such as zona occludens 1-3 (*Zo1-3*) and junctional adhesion molecules 1-3 (*Jam1-3*) (McCarthy et al., 1996; Steed et al., 2010; Tsukita and Furuse, 1999, 2002). Therefore, to demonstrate the presence of tight junctions in the stromal population, we utilized the universal marker occludin (OCLN), which is known to be consistently present in all physiological tight junction apparatuses, formed in mammalian tissues (McCarthy et al., 1996). In the epithelial compartment, OCLN was strongly expressed in tight junctions of normal colonic crypt epithelial cells and, as expected was significantly downregulated in colonic adenocarcinoma cells (Figure 9A). Several colon cancer specimens showed variable OCLN expression in the desmoplastic stroma, ranging from strong to moderate in some areas and weak or absent in others (Figure 9B). In all cases, the OCLN-expressing stromal populations were arranged in peritumoral aggregates or cell cohorts with (myo) fibroblast-like features. We did not observe any cases with focal OCLN expression (Figure 9B).

To confirm that this OCLN-expressing stromal subpopulation was a CAF/myofibroblastic population, further immunohistochemical stains for the myofibroblastic marker α-SMA, the smooth-muscle marker h-caldesmon (CALD), the basement membrane markers laminin-α3 (LAMA3) and laminin-β1 (LAMB1), as well as β-catenin were performed. This showed the OCLN-expressing stromal subpopulation to be α-SMA+, LAMB1+ with only focal CALD expression, supportive of myofibroblastic differentiation (Figure 9C). The mild and focal CALD immunoreactivity could imply the presence of several smooth muscle cells in these regions; however this ectopic presence would be very unlikely, given that the sections examined were clearly present in the submucosa, away from both the *muscularis mucosa* and the *muscularis externa*. The few CALD+, OCLN + stromal cells identified may correspond to a small subpopulation (~11%) of caldesmon + CAFs, occasionally reported in the literature (Xing et al., 2010). As expected, this CAF fraction was negative for markers expressed in certain epithelia, such as LAMA3 and membraneous/nuclear β-catenin (Figure 9C).

4. Discussion

It is well-demonstrated that CAFs are causatively implicated in cancer progression by promoting and supporting the metastatic behavior of cancer cells (De Wever et al., 2008a; Kalluri and Zeisberg, 2006). Additionally, it has been shown that individual fibroblast populations can be discriminated based on their unique gene and protein expression profiles (Chang et al., 2002). In various types of cancer, only specific CAF subpopulations seem to be the key drivers of malignant behaviors. For instance, the fibroblast activation protein (FAP)-overexpressing CAFs seem to be responsible for production of a modified ECM that enhances invasive velocity and directionality of pancreatic cancer cells (Lee et al., 2011). Moreover, Quante et al. (2011) have shown that a specific bone-marrow derived subpopulation of CAFs contributes to the maintenance of the mesenchymal stem cell niche and further promotes tumor growth (Quante et al., 2011). Along the same lines of evidence, we have shown in this study that the OCLN/CLDN11-expressing fibroblasts might represent a specific subpopulation of CAFs, which is dependent upon both the bioavailability of extracellular TGF-β1 and the efficient completion of the TGF-β1 signal transduction pathway within CAFs, in an *in vitro* setting. Specifically, we showed that the cancer cell-produced TGF-β1 may be sufficient for CLDN11-dependent collective migration in CAFs. Consequently, CAFs preferentially migrated non-collectively with stimulation media where TGF-β1 was not present at high concentrations (i.e. SW480/SW620 conditioned media), or was blocked (i.e. inhibition of TGF-β1 in HT29 conditioned media by specific neutralizing antibodies).

TGF-β1 is the major-reported cytokine, implicated in the paracrine signaling module between cancer cells and CAFs and responsible for the fibroblast-to-myofibroblast transdifferentiation program (Ronnov-Jessen and Petersen, 1993). It is secreted as a latent complex stored in the extracellular matrix. Subsequent proteolytic activity and other non-proteolytic mechanisms, driven by the CAFs, result in the availability of bioactive TGF-β1 (Kalluri and Zeisberg, 2006). The levels of TGF-β1 are significantly elevated in many human cancers (Norgaard et al., 1995), including colorectal carcinomas (Tsushima et al., 1996). The intensity and degree of desmoplasia in various types of cancer have been directly associated with the TGF-β1 production by the cancer cells (Kunz-Schughart and Knuechel, 2002). TGF-β1 has been demonstrated to act as chemotactic agent for fibroblasts. Interestingly, CAF migration appears to be regulated by TGF-β1 in a dose-dependent manner, as has already been shown by others (Denys et al., 2008; Hawinkels et al., 2009), as well as the current study. Therefore, TGF-β1 signaling appears to particularly be a rate-limiting step for the collectivity of the CAF migratory pattern. We believe that it was for this reason that the application of the tight junction inhibitor MEHP, especially in the presence of high TGF-β1 concentrations, facilitated full attenuation of the collective nature by which colonic CAFs migrated.

Interestingly, the HT29 colon cancer cell line is highly tumorigenic and induces cancer in mouse xenografts (Oliver et al., 2008). Factors secreted from this particular cell line,

including TGF-β1, have been shown in this study to induce an aberrant stromal response in fibroblasts, specifically causing myofibroblastic transdifferentiation and collective migration *in vitro*. Thus, it is tempting to speculate one of the possible reasons this cell line may induce tumors in these xenografts, in contrast to the SW480 and SW620 ones, could be due to its ability to stimulate a tumor-promoting desmoplastic stromal response in the adjacent normal tissues. To our knowledge though, no one has yet investigated the desmoplastic nature (if indeed any) of HT29-induced cancers in such xenografts.

However there is some debating literature (Fang et al., 2011; Franco et al., 2011; Li et al., 2011; Meng et al., 2011), suggesting that CAFs lose the ability to propagate the TGF-β signal transduction pathway because of loss of TGF-β receptor type II. Moreover, the overexpression of Caveolin-1, a molecule known to inhibit the function of TGF-β receptor (Pavlides et al., 2011), has been reported in CAFs/myofibroblasts in many types of cancer or fibrotic diseases (Kim et al., 2011; Xia et al., 2010). Additional evidence of absence of TGF-β signaling in CAFs arises from studies focused on the restricted bioavailability of active TGF-β at the tumor microenvironment. Although TGF-β is constantly secreted in the cancer microenvironment by cancer cells, subsequent proteolytic activity and ECM remodeling results in the sequestering of the active form of the ligand (Hanahan and Weinberg, 2011). Of note, the probable serine proteases-1, -2 and -3 (HTRA-1, -2, and -3), typically overexpressed at the cancer invasion margins (Narkiewicz et al., 2009), are capable of sequestering TGF-β1 through ECM remodeling activity (Tocharus et al., 2004). As a consequence, CAFs retain their myofibroblastic phenotype through alternative signaling pathways, such as possibly the PDGF signaling pathway and not through TGF-β (Kalluri and Zeisberg, 2006).

Our immunohistochemical data are consistent with the fact that CAFs express the tight junction protein occludin, thus validating our hypothesis and working model regarding the collective nature of CAF migration in desmoplastic lesions in cancer (Karagiannis et al., 2012b). In general, tight junctions seal neighboring epithelial or endothelial cells, regulating the paracellular transportation of molecules and ions in between. Tight junctions have also been demonstrated to provide epithelial or apico-basolatelar polarity to the cells that do express them. Tight junction formation and expression has been described as a hallmark of epithelial cells and their subsequent loss from cancer cells tends to be considered as a direct effect of EMT (De Wever et al., 2008b). However, the expression of tight junction molecules in myofibroblasts during wound healing has been noted early (Farber and Rubin, 1990), whereby it has been speculated that CAFs may utilize a tight junction machinery to obtain collective configuration and migrate in cohorts (Karagiannis et al., 2012b).

Tight junctions are currently established as playing causative and regulatory roles in various types of cancer, and insights into their regulation are beginning to emerge. For instance, Runkle et al. (2011) have suggested a TTF1-dependent transcriptional regulation of OCLN in lung cancer (Runkle et al., 2011). More interestingly, recent studies suggest that OCLN may comprise signaling properties as well, as it was found capable of inducing apoptotic signals *per se*, in cases of tight junction disruption (Beeman et al., 2013, 2009). Therefore, these novel avenues regarding the regulation of colorectal and other cancers by tight junctions need to be clarified and thoroughly investigated in the future.

Here, we established for the first time the paracrine axis TGFB1-OCLN/CLDN11 between cancer cells and CAFs. This axis may serve as a proof of concept paracrine signaling module for the recent working hypothesis, stating that the recruitment of CAFs by the cancer cells does not lead to the deterministic generation of one specific CAF population. On the contrary, it seems that the CAF migratory gene/protein expression machinery is context-dependent, varying from totally individual to collective configuration, since it is regulated by the permissive microenvironment of a TGF-β1-secreting cancer cell subpopulation.

5. Author contributions

Conceptualized study: GSK; Designed, performed and interpreted *in-vitro* experiments: GSK, NM, PS; Designed, performed and interpreted proteomics/bioinformatics experiments: GSK, CKJC, IB; Designed, performed and interpreted IHC studies: GSK, DFS, AG, BM, RK, RHR; Wrote manuscript: GSK and EPD; Revised Manuscript: all authors.

6. Conflicts of interest

None.

Acknowledgments

George S. Karagiannis is supported by University Health Network and Mount Sinai Hospital, Toronto, ON, Canada. The authors kindly thank Chris Smith for technical assistance in mass spectrometry, Antoninus Soosaipillai for technical and laboratory assistance, and Maria Pavlou, Shalini Makawita, Yiannis Prassas and Uros Kuzmanov for helpful suggestions.

Appendix A. Supplementary data

Supplementary data related to this article can be found at http://dx.doi.org/10.1016/j.molonc.2013.10.008.

REFERENCES

Beeman, N., Webb, P.G., Baumgartner, H.K., 2013. Occludin is required for apoptosis when claudin-claudin interactions are disrupted. Cell Death Dis. 3, e273.

Beeman, N.E., Baumgartner, H.K., Webb, P.G., Schaack, J.B., Neville, M.C., 2009. Disruption of occludin function in polarized epithelial cells activates the extrinsic pathway of apoptosis leading to cell extrusion without loss of transepithelial resistance. BMC Cell Biol. 10, 85.

Bertos, N.R., Park, M., 2011. Breast cancer – one term, many entities? J. Clin. Invest. 121, 3789–3796.
Blaschuk, O.W., Oshima, T., Gour, B.J., Symonds, J.M., Park, J.H., Kevil, C.G., et al., 2002. Identification of an occludin cell adhesion recognition sequence. Inflammation 26, 193–198.
Brenmoehl, J., Miller, S.N., Hofmann, C., Vogl, D., Falk, W., Scholmerich, J., et al., 2009. Transforming growth factor-beta 1 induces intestinal myofibroblast differentiation and modulates their migration. World J. Gastroenterol. 15, 1431–1442.
Chang, H.Y., Chi, J.T., Dudoit, S., Bondre, C., van de Rijn, M., Botstein, D., et al., 2002. Diversity, topographic differentiation, and positional memory in human fibroblasts. Proc. Natl. Acad. Sci. U S A 99, 12877–12882.
Chiba, K., Kondo, Y., Yamaguchi, K., Miyake, H., Fujisawa, M., 2011. Inhibition of Claudin-11 and occludin expression in rat Sertoli cells by mono-(2-ethylhexyl) phthalate through p44/42 mitogen-activated protein kinase pathway. J. Androl. 33, 368–374.
Clavel, C., Polette, M., Doco, M., Binninger, I., Birembaut, P., 1992. Immunolocalization of matrix metallo-proteinases and their tissue inhibitor in human mammary pathology. Bull. Cancer 79, 261–270.
Collier, T.S., Sarkar, P., Franck, W.L., Rao, B.M., Dean, R.A., Muddiman, D.C., 2010. Direct comparison of stable isotope labeling by amino acids in cell culture and spectral counting for quantitative proteomics. Anal. Chem. 82, 8696–8702.
Cox, J., Mann, M., 2008. MaxQuant enables high peptide identification rates, individualized p.p.b.-range mass accuracies and proteome-wide protein quantification. Nat. Biotechnol. 26, 1367–1372.
Cox, J., Matic, I., Hilger, M., Nagaraj, N., Selbach, M., Olsen, J.V., et al., 2009. A practical guide to the MaxQuant computational platform for SILAC-based quantitative proteomics. Nat. Protoc. 4, 698–705.
De Wever, O., Demetter, P., Mareel, M., Bracke, M., 2008a. Stromal myofibroblasts are drivers of invasive cancer growth. Int. J. Cancer 123, 2229–2238.
De Wever, O., Pauwels, P., De Craene, B., Sabbah, M., Emami, S., Redeuilh, G., et al., 2008b. Molecular and pathological signatures of epithelial-mesenchymal transitions at the cancer invasion front. Histochem. Cell Biol. 130, 481–494.
Denys, H., Derycke, L., Hendrix, A., Westbroek, W., Gheldof, A., Narine, K., et al., 2008. Differential impact of TGF-beta and EGF on fibroblast differentiation and invasion reciprocally promotes colon cancer cell invasion. Cancer Lett. 266, 263–274.
Desmouliere, A., Geinoz, A., Gabbiani, F., Gabbiani, G., 1993. Transforming growth factor-beta 1 induces alpha-smooth muscle actin expression in granulation tissue myofibroblasts and in quiescent and growing cultured fibroblasts. J. Cell Biol. 122, 103–111.
Dey, T., Mann, M.C., Goldmann, W.H., 2011. Comparing mechano-transduction in fibroblasts deficient of focal adhesion proteins. Biochem. Biophys. Res. Commun. 413, 541–544.
Direkze, N.C., Hodivala-Dilke, K., Jeffery, R., Hunt, T., Poulsom, R., Oukrif, D., et al., 2004. Bone marrow contribution to tumor-associated myofibroblasts and fibroblasts. Cancer Res. 64, 8492–8495.
Elenbaas, B., Weinberg, R.A., 2001. Heterotypic signaling between epithelial tumor cells and fibroblasts in carcinoma formation. Exp. Cell Res. 264, 169–184.
Etienne-Manneville, S., 2008. Polarity proteins in migration and invasion. Oncogene 27, 6970–6980.
Fang, W.B., Jokar, I., Chytil, A., Moses, H.L., Abel, T., Cheng, N., 2011. Loss of one Tgfbr2 allele in fibroblasts promotes metastasis in MMTV: polyoma middle T transgenic and transplant mouse models of mammary tumor progression. Clin. Exp. Metastasis 28, 351–366.
Farber, J.L., Rubin, E., 1990. Essential Pathology, vol. xiv. J.B. Lippincott Co, Philadelphia, p. 850.
Finak, G., Bertos, N., Pepin, F., Sadekova, S., Souleimanova, M., Zhao, H., et al., 2008. Stromal gene expression predicts clinical outcome in breast cancer. Nat. Med. 14, 518–527.
Finak, G., Sadekova, S., Pepin, F., Hallett, M., Meterissian, S., Halwani, F., et al., 2006. Gene expression signatures of morphologically normal breast tissue identify basal-like tumors. Breast Cancer Res. 8, R58.
Franco, O.E., Jiang, M., Strand, D.W., Peacock, J., Fernandez, S., Jackson 2nd, R.S., et al., 2011. Altered TGF-beta signaling in a subpopulation of human stromal cells promotes prostatic carcinogenesis. Cancer Res. 71, 1272–1281.
Gustafson, C.E., Wilson, P.J., Lukeis, R., Baker, E., Woollatt, E., Annab, L., et al., 1996. Functional evidence for a colorectal cancer tumor suppressor gene at chromosome 8p22-23 by monochromosome transfer. Cancer Res. 56, 5238–5245.
Hanahan, D., Weinberg, R.A., 2011. Hallmarks of cancer: the next generation. Cell 144, 646–674.
Hawinkels, L.J., Verspaget, H.W., van der Reijden, J.J., van der Zon, J.M., Verheijen, J.H., Hommes, D.W., et al., 2009. Active TGF-beta1 correlates with myofibroblasts and malignancy in the colorectal adenoma-carcinoma sequence. Cancer Sci. 100, 663–670.
Heldin, C.H., Rubin, K., Pietras, K., Ostman, A., 2004. High interstitial fluid pressure – an obstacle in cancer therapy. Nat. Rev. Cancer 4, 806–813.
Kalluri, R., Weinberg, R.A., 2009. The basics of epithelial-mesenchymal transition. J. Clin. Invest. 119, 1420–1428.
Kalluri, R., Zeisberg, M., 2006. Fibroblasts in cancer. Nat. Rev. Cancer 6, 392–401.
Karagiannis, G.S., Berk, A., Dimitromanolakis, A., Diamandis, E.P., 2013. Enrichment map profiling of the cancer invasion front suggests regulation of colorectal cancer progression by the bone morphogenetic protein antagonist, gremlin-1. Mol. Oncol. 7, 826–839.
Karagiannis, G.S., Petraki, C., Prassas, I., Saraon, P., Musrap, N., Dimitromanolakis, A., et al., 2012a. Proteomic signatures of the desmoplastic invasion front reveal collagen type XII as a marker of myofibroblastic differentiation during colorectal cancer metastasis. Oncotarget 3, 267–285.
Karagiannis, G.S., Poutahidis, T., Erdman, S.E., Kirsch, R., Riddell, R.H., Diamandis, E.P., 2012b. Cancer-associated fibroblasts drive the progression of metastasis through both paracrine and mechanical pressure on cancer tissue. Mol. Cancer Res. 10, 1403–1418.
Kim, D., Kim, H., Koo, J.S., 2011. Expression of caveolin-1, caveolin-2 and caveolin-3 in thyroid cancer and stroma. Pathobiology 79, 1–10.
Kunz-Schughart, L.A., Knuechel, R., 2002. Tumor-associated fibroblasts (part I): active stromal participants in tumor development and progression? Histol. Histopathol. 17, 599–621.
Lee, H.O., Mullins, S.R., Franco-Barraza, J., Valianou, M., Cukierman, E., Cheng, J.D., 2011. FAP-overexpressing fibroblasts produce an extracellular matrix that enhances invasive velocity and directionality of pancreatic cancer cells. BMC Cancer 11, 245.
Leibovitz, A., Stinson, J.C., McCombs 3rd, W.B., McCoy, C.E., Mazur, K.C., Mabry, N.D., 1976. Classification of human colorectal adenocarcinoma cell lines. Cancer Res. 36, 4562–4569.
Lewis, M.P., Lygoe, K.A., Nystrom, M.L., Anderson, W.P., Speight, P.M., Marshall, J.F., et al., 2004. Tumour-derived TGF-beta1 modulates myofibroblast differentiation and promotes HGF/SF-dependent invasion of squamous carcinoma cells. Br. J. Cancer 90, 822–832.
Li, X., Sterling, J.A., Fan, K.H., Vessella, R.L., Shyr, Y., Hayward, S.W., et al., 2011. Loss of TGF-beta responsiveness in

prostate stromal cells alters chemokine levels and facilitates the development of mixed osteoblastic/osteolytic bone lesions. Mol. Cancer Res. 10, 494–503.
Mazaud-Guittot, S., Meugnier, E., Pesenti, S., Wu, X., Vidal, H., Gow, A., et al., 2010. Claudin 11 deficiency in mice results in loss of the Sertoli cell epithelial phenotype in the testis. Biol. Reprod. 82, 202–213.
McCarthy, K.M., Skare, I.B., Stankewich, M.C., Furuse, M., Tsukita, S., Rogers, R.A., et al., 1996. Occludin is a functional component of the tight junction. J. Cell Sci. 109 (Pt 9), 2287–2298.
Meng, W., Xia, Q., Wu, L., Chen, S., He, X., Zhang, L., et al., 2011. Downregulation of TGF-beta receptor types II and III in oral squamous cell carcinoma and oral carcinoma-associated fibroblasts. BMC Cancer 11, 88.
Morita, K., Sasaki, H., Fujimoto, K., Furuse, M., Tsukita, S., 1999. Claudin-11/OSP-based tight junctions of myelin sheaths in brain and Sertoli cells in testis. J. Cell Biol. 145, 579–588.
Narkiewicz, J., Lapinska-Szumczyk, S., Zurawa-Janicka, D., Skorko-Glonek, J., Emerich, J., Lipinska, B., 2009. Expression of human HtrA1, HtrA2, HtrA3 and TGF-beta1 genes in primary endometrial cancer. Oncol. Rep. 21, 1529–1537.
Navab, R., Strumpf, D., Bandarchi, B., Zhu, C.Q., Pintilie, M., Ramnarine, V.R., et al., 2011. Prognostic gene-expression signature of carcinoma-associated fibroblasts in non-small cell lung cancer. Proc. Natl. Acad. Sci. U S A 108, 7160–7165.
Norgaard, P., Hougaard, S., Poulsen, H.S., Spang-Thomsen, M., 1995. Transforming growth factor beta and cancer. Cancer Treat. Rev. 21, 367–403.
Oliver, P.G., LoBuglio, A.F., Zinn, K.R., Kim, H., Nan, L., Zhou, T., et al., 2008. Treatment of human colon cancer xenografts with TRA-8 anti-death receptor 5 antibody alone or in combination with CPT-11. Clin. Cancer Res. 14, 2180–2189.
Ong, S.E., Blagoev, B., Kratchmarova, I., Kristensen, D.B., Steen, H., Pandey, A., et al., 2002. Stable isotope labeling by amino acids in cell culture, SILAC, as a simple and accurate approach to expression proteomics. Mol. Cell Proteomics 1, 376–386.
Pavlides, S., Tsirigos, A., Vera, I., Flomenberg, N., Frank, P.G., Casimiro, M.C., et al., 2011. Loss of stromal caveolin-1 leads to oxidative stress, mimics hypoxia and drives inflammation in the tumor microenvironment, conferring the “reverse Warburg effect”: a transcriptional informatics analysis with validation. Cell Cycle 9, 2201–2219.
Petersen, O.W., Lind Nielsen, H., Gudjonsson, T., Villadsen, R., Ronnov-Jessen, L., Bissell, M.J., 2001. The plasticity of human breast carcinoma cells is more than epithelial to mesenchymal conversion. Breast Cancer Res. 3, 213–217.
Petersen, O.W., Nielsen, H.L., Gudjonsson, T., Villadsen, R., Rank, F., Niebuhr, E., et al., 2003. Epithelial to mesenchymal transition in human breast cancer can provide a nonmalignant stroma. Am. J. Pathol. 162, 391–402.
Popanda, O., Zheng, C., Magdeburg, J.R., Buttner, J., Flohr, T., Hagmuller, E., et al., 2000. Mutation analysis of replicative genes encoding the large subunits of DNA polymerase alpha and replication factors A and C in human sporadic colorectal cancers. Int. J. Cancer 86, 318–324.
Potenta, S., Zeisberg, E., Kalluri, R., 2008. The role of endothelial-to-mesenchymal transition in cancer progression. Br. J. Cancer 99, 1375–1379.
Prassas, I., Karagiannis, G.S., Batruch, I., Dimitromanolakis, A., Datti, A., Diamandis, E.P., 2011. Digitoxin-induced cytotoxicity in cancer cells is mediated through distinct kinase and interferon signaling networks. Mol. Cancer Ther. 10, 2083–2093.
Quante, M., Tu, S.P., Tomita, H., Gonda, T., Wang, S.S., Takashi, S., et al., 2011. Bone marrow-derived myofibroblasts contribute to the mesenchymal stem cell niche and promote tumor growth. Cancer Cell 19, 257–272.
Ronnov-Jessen, L., Petersen, O.W., 1993. Induction of alpha-smooth muscle actin by transforming growth factor-beta 1 in quiescent human breast gland fibroblasts. Implications for myofibroblast generation in breast neoplasia. Lab Invest. 68, 696–707.
Rorth, P., 2009. Collective cell migration. Annu. Rev. Cell Dev. Biol. 25, 407–429.
Runkle, E.A., Rice, S.J., Qi, J., Masser, D., Antonetti, D.A., Winslow, M.M., et al., 2011. Occludin is a direct target of thyroid transcription factor-1 (TTF-1/NKX2-1). J. Biol. Chem. 287, 28790–28801.
Russo, F.P., Alison, M.R., Bigger, B.W., Amofah, E., Florou, A., Amin, F., et al., 2006. The bone marrow functionally contributes to liver fibrosis. Gastroenterology 130, 1807–1821.
Scheel, C., Eaton, E.N., Li, S.H., Chaffer, C.L., Reinhardt, F., Kah, K.J., et al., 2011. Paracrine and autocrine signals induce and maintain mesenchymal and stem cell states in the breast. Cell 145, 926–940.
Serini, G., Gabbiani, G., 1999. Mechanisms of myofibroblast activity and phenotypic modulation. Exp. Cell Res. 250, 273–283.
Shi, Z.R., Tsao, D., Kim, Y.S., 1983. Subcellular distribution, synthesis, and release of carcinoembryonic antigen in cultured human colon adenocarcinoma cell lines. Cancer Res. 43, 4045–4049.
Steed, E., Balda, M.S., Matter, K., 2010. Dynamics and functions of tight junctions. Trends Cell Biol. 20, 142–149.
Tingstrom, A., Heldin, C.H., Rubin, K., 1992. Regulation of fibroblast-mediated collagen gel contraction by platelet-derived growth factor, interleukin-1 alpha and transforming growth factor-beta 1. J. Cell Sci. 102 (Pt 2), 315–322.
Tiwari-Woodruff, S.K., Buznikov, A.G., Vu, T.Q., Micevych, P.E., Chen, K., Kornblum, H.I., et al., 2001. OSP/claudin-11 forms a complex with a novel member of the tetraspanin super family and beta1 integrin and regulates proliferation and migration of oligodendrocytes. J. Cell Biol. 153, 295–305.
Tocharus, J., Tsuchiya, A., Kajikawa, M., Ueta, Y., Oka, C., Kawaichi, M., 2004. Developmentally regulated expression of mouse HtrA3 and its role as an inhibitor of TGF-beta signaling. Dev. Growth Differ. 46, 257–274.
Tsukita, S., Furuse, M., 1999. Occludin and claudins in tight-junction strands: leading or supporting players? Trends Cell Biol. 9, 268–273.
Tsukita, S., Furuse, M., 2002. Claudin-based barrier in simple and stratified cellular sheets. Curr. Opin. Cell Biol. 14, 531–536.
Tsushima, H., Kawata, S., Tamura, S., Ito, N., Shirai, Y., Kiso, S., et al., 1996. High levels of transforming growth factor beta 1 in patients with colorectal cancer: association with disease progression. Gastroenterology 110, 375–382.
Xia, H., Khalil, W., Kahm, J., Jessurun, J., Kleidon, J., Henke, C.A., 2010. Pathologic caveolin-1 regulation of PTEN in idiopathic pulmonary fibrosis. Am. J. Pathol. 176, 2626–2637.
Xing, F., Saidou, J., Watabe, K., 2010. Cancer associated fibroblasts (CAFs) in tumor microenvironment. Front Biosci. 15, 166–179.
Zanotti, S., Gibertini, S., Mora, M., 2010. Altered production of extra-cellular matrix components by muscle-derived Duchenne muscular dystrophy fibroblasts before and after TGF-beta1 treatment. Cell Tissue Res. 339, 397–410.